Grana, 2016
Vol. 55, No. 1, 71–100, http://dx.doi.org/10.1080/00173134.2015.1120343

Taylor & Francis
Taylor & Francis Group

Steppe development on the Northern Tibetan Plateau inferred from Paleogene ephedroid pollen

FANG HAN[1,2], CATARINA RYDIN [3], KRISTINA BOLINDER[3], GUILLAUME DUPONT-NIVET[4,5], HEMMO A. ABELS[6], ANDREAS KOUTSODENDRIS[7], KEXIN ZHANG[8] & CARINA HOORN[2]

[1]*School of Earth Science, East China University of Technology, Nanchang, China,* [2]*Institute for Biodiversity and Ecosystem Dynamics, University of Amsterdam, Amsterdam, The Netherlands,* [3]*Department of Ecology, Environment and Plant Sciences, Stockholm University, Stockholm, Sweden,* [4]*Institute of Earth and Environmental Science, Potsdam University, Potsdam-Golm, Germany,* [5]*Géosciences Rennes, Université de Rennes 1, Rennes, France,* [6]*Department of Earth Sciences, Utrecht University, Utrecht, The Netherlands,* [7]*Paleoenvironmental Dynamics Group, Institute of Earth Sciences, Heidelberg University, Heidelberg, Germany,* [8]*University of Geosciences, Wuhan, China*

Abstract
Steppe vegetation represents a key marker of past Asian aridification and is associated with monsoonal intensification. Little is, however, known about the origin of this pre-Oligocene vegetation, its specific composition and how it changed over time and responded to climatic variations. Here, we describe the morphological characters of Ephedraceae pollen in Eocene strata of the Xining Basin and compare the pollen composition with the palynological composition of Late Cretaceous and Paleocene deposits of the Xining Basin and the Quaternary deposits of the Qaidam Basin. We find that the Late Cretaceous steppe was dominated by *Gnetaceaepollenites*; in the transition from the Cretaceous to the Paleocene, *Gnetaceaepollenites* became extinct and *Ephedripites* subgenus *Ephedripites* dominated the flora with rare occurrences of *Ephedripites* subgen. *Distachyapites*; the middle to late Eocene presents a strong increase of *Ephedripites* subgen. *Distachyapites*; and the Quaternary/Recent is marked by a significantly lower diversity of Ephedraceae (and Nitrariaceae) compared to the Eocene. In the modern landscape of China, only a fraction of the Paleogene species diversity of Ephedraceae remains and we propose that these alterations in Ephedreaceae composition occurred in response to the climatic changes at least since the Eocene. In particular, the strong Eocene monsoons that enhanced the continental aridification may have played an important role in the evolution of *Ephedripites* subgen. *Distachyapites* triggering an evolutionary shift to wind-pollination in this group. Conceivably, the Ephedraceae/Nitrariaceae dominated steppe ended during the Eocene/Oligocene climatic cooling and aridification, which favoured other plant taxa.

Keywords: *pollen morphology, Eocene, climate,* Ephedripites, Distachyapites, Gnetaceaepollenites, *monsoon*

The steppe vegetation of China is, similar to the steppe in the eastern extent of Europe, mainly composed of Poaceae, Asteraceae and Chenopodiaceae with minor amounts of Ephedraceae and Nitrariaceae including taxa such as *Stipa, Festuca, Cleistogenes, Artemisia* and *Sanguisorba* (Sun & Wang 2005). The vegetation in the desert regions of northwest China is partially influenced by the East Asian monsoon system and, contrary to other Chinese steppes, mainly composed of *Salsola, Anabasis, Suaeda* and *Artemisia*. In this region, the Nitrariaceae (*Nitraria*) and the Ephedraceae occur in much lower percentages than other xeromorphic taxa (Wu 1980; Zhang et al. 2007).

Today, there are only five recognised species of Nitrariaceae and 14 recognised species of *Ephedra* in northern and northwest China (Fu et al. 1999; Yang 2002; Li 2008). However, during the Late Cretaceous–Paleogene, the palynological fossil record shows that Ephedraceae and Nitrariaceae were both

Correspondence: Fang Han, School of Earth Science, East China University of Technology, Nanchang, 330013, China. E-mail: *fanghan@ecit.cn*

(Received 31 March 2015; accepted 2 October 2015)

widely distributed and diverse and dominating steppe vegetation of China (Li 1989; Shaw 1998; Wang et al. 1999; Yu et al. 2003; Wu et al. 2006; Duan et al. 2007; Li et al. 2008; Hoorn et al. 2012; Miao et al. 2013a; Miao et al. 2015). According to Song (1999), based on pollen, more than 100 species of Ephedraceae are reported for China during the late Cretaceous–Cenozoic. The relatively high diversity and abundance of polyplicate fossil pollen grains (ephedroid pollen, see later) are characteristic not only for China, but also globally during the Late Cretaceous–Cenozoic (Figure 1; Wodehouse 1933; Cookson 1956; Gray 1960; Scott 1960; Ghosh et al. 1963; Muller 1968; Srivastava 1968; Hochuli 1981; Chlonova et al. 1994; Takahashi et al. 1995; Dino et al. 1999; Dilcher et al. 2005; Akkiraz et al. 2008; Narváez & Sabino 2008; Abubakar et al. 2011).

But when did the steppe-desert assemblage change from an Ephedraceae and Nitrariaceae dominated composition to a vegetation dominated by Poaceae, Asteraceae and Chenopodiaceae? There are different views on this. The pollen record from the Qaidam Basin and the Linxia Basin shows that the Chenopodiaceae already dominated the steppe vegetation in the Oligocene (Zhu et al. 1985; Ma et al. 1998; Wang & Shu 2013). Miao et al. (2011) combined Ephedraceae records from the Xining Basin with that of four other sedimentary basins in north-western China (Tarim, Qaidam, Junggar and Lunpola basins), and came to the conclusion that the abundance of Ephedraceae was high during the Paleocene and Eocene and decreased gradually from the middle Eocene onwards. In contrast, Song et al. (2008) stated that Nitrariaceae and Ephedraceae rapidly increased in the middle–late Eocene and dominated the steppe vegetation in northwest China during the Oligocene only to be replaced by the *Artemisia* and Chenopodiaceae vegetation in the late Oligocene. In addition, pollen records from the Xining-Minhe Basin show that *Ephedripites* dominated the pollen assemblages from the Senonian (Late Cretaceous), and reached their peak during the Paleocene (up to 60%), decreased in early–middle Oligocene and finally were replaced by Chenopodiaceae in the late Oligocene (Sun et al. 1984; Wang et al. 1990; Ma et al. 1998). Previous studies in the Tarim Basin reveal that, while *Ephedripites* dominated the late Paleocene–Oligocene, Asteraceae and Chenopodiaceae were abundant in the Miocene (Wang et al. 1990; Zhang & Zhan 1991).

Until now, most palaeo-palynological studies of Ephedraceae have focused on fluctuations in relative abundance through time. Few studies address the morphological differences among pollen types and studies on how ephedroids evolved throughout their long evolutionary history from the Cretaceous to the Present are limited. Furthermore, due to the limited resolution of light microscopy (LM), earlier descriptions of fossil polyplicate pollen types did often not mention details of the psedosulci.

To contribute to a better understanding of the evolution of the steppe development, we here focus on the Cretaceous to Paleogene records in northwest China, with particular emphasis on the Eocene record in the Xining Basin. We illustrate key taxa with scanning electron microscopy (SEM) and LM photography and describe key morphological features. Finally, we compare this record with that of the Quaternary of the nearby Qaidam Basin (Figure 2) and highlight implications for improved understanding of steppe evolution.

Study area

The study area is located north of the Tibetan Plateau, which provides key records of the aridification of Central Asia and the evolution of the East Asian monsoon system in response to changes in global climate and regional land-sea distribution (Kutzbach et al. 1993; Liu & Yin 2002; Davis 2005; Leier et al. 2005; Dupont-Nivet et al. 2008; Paytan 2012; Quan et al. 2012; Wu et al. 2012; Lu & Guo 2013; Li et al. 2014; Bosboom et al. 2014b). Our study areas are situated in the Xining and Qaidam basins and form part of the Qinghai province, China (Figure 2). These two basins both include continuous records of the variations in climate aridity at least since the Eocene (Sun & Wang 2005; Song et al. 2008; Abels et al. 2011). As such, the available terrestrial sedimentary sequences from these settings (Xiao et al. 2010; Abels et al. 2011; Wang et al. 2012; Song et al. 2013) provide the ideal material to better understand the evolution of steppe vegetation during the Cenozoic.

Nowadays, there are eight recognised species of *Ephedra* in the study area. These include *Ephedra przewalskii* Stapf, *E. intermedia* Schrenk ex C.A. Mey., *E. gerardiana* Wall. ex C.A. Mey., *E. equisetina* Bunge, *E. monosperma* C.A. Mey. and *E. minuta* Florin (distributed within an altitudinal range of 300–3700 m to 3000–5300 m), *E. sinica* Stapf (often found in mountain slopes between 700–1600 m) and *E. distachya* L. (mainly found in sandy places and rocky mountain slopes below 900 m; Fu et al. 1999).

The Xining Basin is located at the north-eastern margin of the Tibetan Plateau in the northern Qinghai province, at an elevation of ~2000 m and is characterised by a cold and semi-arid climate affected by the East Asian monsoons. The Cretaceous study site is situated in east Xining (36° 35′ N, 101° 54′ E) and the Eocene sites are located in Shuiwan (36° 39′ N, 101° 52′

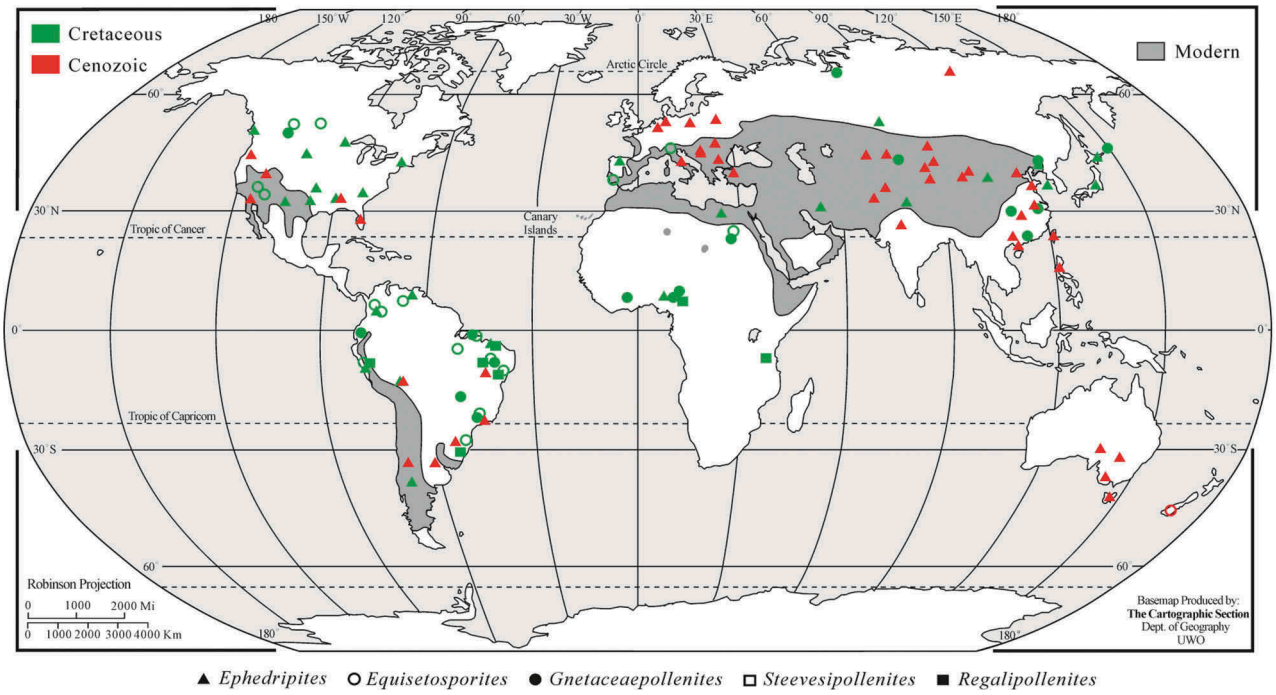

Figure 1. Global distribution of ephedroid pollen in the Cretaceous–Cenozoic. Modified after Caveney et al. (2001) and Dilcher et al. (2005) with ephedroid pollen locations from reference list (Attachment 1) and from Garcia et al. (2016). Noteworthy is the extensive distribution of ephedroid pollen in the Cretaceous compared to the present.

E) and Tiefo, near the city of Xining (Dai et al. 2006; Dupont-Nivet et al. 2007, 2008; Abels et al. 2011; Hoorn et al. 2012; Bosboom et al. 2014a). All these sites are well-documented and especially the middle to late Eocene sections are well-dated with magnetostratigraphy (Figure 3; Horton et al. 2004; Dupont-Nivet et al. 2007; Abels et al. 2012; Bosboom et al. 2014a). Palynological samples from these sites were processed and analysed to detect changes in palynological composition (Hoorn et al. 2012; Bosboom et al. 2014a).

The Qaidam Basin is situated to the west of the Xining Basin (northwest Qinghai province) at an elevation of ~3000 m and is characterised by a cold arid to semi-arid climate. The Quaternary samples were taken from the SG-1 core, which was retrieved in 2008 in the western Qaidam Basin (38° 24′ 35″ N, 92° 30′ 33″ E). The core sediments span the entire Quaternary based on a robust age model obtained through magnetostratigraphy, optically stimulated luminescence (OSL) dating and orbital tuning (Figure 3; Zhang et al. 2012; Herb et al. 2015).

Material and methods

Sample processing

The Cretaceous–Early Palaeogene samples were previously processed by Horton et al. (2004) and two of them (O2X 351 and O2X 535) were reprocessed at the University of Amsterdam (UvA), The Netherlands, in order to select single grains for SEM photography. Samples from the Shuiwan section (13 samples) and the Tiefo section (seven samples) were previously processed at the Vrije Universiteit (VU), Amsterdam, The Netherlands, and three additional samples from theTiefo section were processed at UvA (Hoorn et al. 2012). Methods are explained in Hoorn et al. (2012)

Figure 2. Location of the study area (modified after Bosboom et al. 2014b).

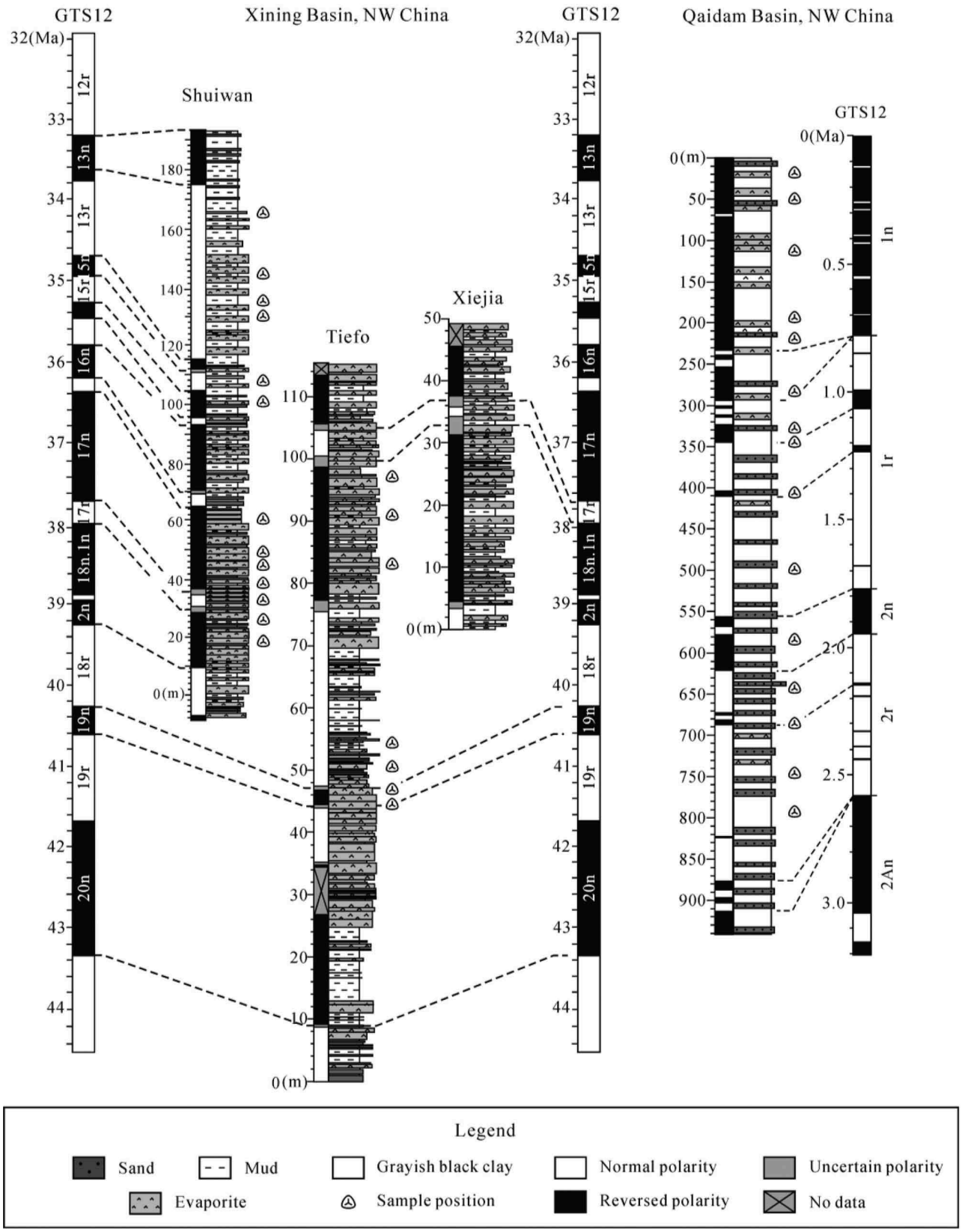

Figure 3. Magnetostratigraphy and sample position of the studied section in the Xining Basin and of the SG-1 core from the Qaidam Basin. All the pollen samples were used for morphological study, but it should be noted that the samples from the SG-1 core were not included in the percentage diagrams. The lithological column of Shuiwan section was modified after Abels et al. (2011) and Hoorn et al. (2012); the lithological column of Tiefo and Xiejia section were modified after Bosboom et al. (2014b). The lithological column of SG-1 core was modified after Zhang et al. (2012) and Herb et al. (2015).

and Bosboom et al. (2014a). The Quaternary samples (19 samples) from the SG-1 core were processed with standard palynological techniques including freeze drying, weighing, treating with hydrochloric acid (HCl) (30%) and hydrofluoric acid (HF) (40%), and sieving (10 μm nylon mesh) in an ultrasonic bath.

Pollen was observed using a Leica DMLB light microscope (100× objective, 10× eyepieces) and the microphotographs were photographed by Nomarski Differential Interference Contrast (DIC) microscopy (Bercovici et al. 2009). While making the photographs, the varying *z*-axis was recorded and images were later combined through manual z-stacking in Photoshop. This stacking technique combines different layers to provide a sense of depth to the images, with a result comparable to three-dimensional (3D) photography.

Single grains of polyplicate pollen were first photographed using LM at a magnification of 40× and then evaporated onto aluminium stubs using the single grain technique (Hesse et al. 2009). The pollen was sputter-coated with gold (40 s at 10 mA) and studied under a JEOL JSM-7401 F scanning electron microscope at 2.0 kV at the Department of Materials and Environmental Chemistry, Stockholm University, Stockholm, Sweden. Length of the polar and the equatorial axes was measured directly on the SEM screen and the *P*/*E* ratio was obtained. The number of plicae was counted on the visible side of the grain and multiplied by two to obtain the total number of plicae.

Pollen grains were identified using the 'Genera File of Fossil Pollen and Spores' (Jansonius & Hills 1980) and other references (Krutzsch 1961, 1970; Stover 1964; Song 1978, 1999; De Lima 1979a; Sun & He 1980; Zhu et al. 1985; Zhang & Zhan 1991). Terminology follows Punt et al. (2007) and the pollen description generally follows the format outlined by Jaramillo and Dilcher (2001). At least ten grains (30 for average, 150 for maximum) were measured for each studied species. The counted specimens are represented in cumulative and composition diagrams constructed with the program Tilia (Grimm 1987). The complete palynological assemblage was previously published in Hoorn et al. (2012) and Bosboom et al. (2014a).

Results

Taxonomic review

According to the current pollen classification of the Cenozoic in China, ephedroid pollen is represented by three genera (*Ephedripites, Regalipollenites, Steevesipollenites*) and three subgenera (*E.* subgen. *Ephedripites*, *E.* subgen. *Distachyapites*, *E.* subgen. *Spiralipites*; Song 1999). It should also be mentioned that *Schizaeoisporites* is frequently thought of as a spore with narrow or broad plicae without fusion (Song 1999) and is often confused with *Gnetaceaepollenites*.

Thiergart (1938) first described the morphological characteristics of ephedroid pollen and erected *Gnetaceaepollenites* to include all ephedroid pollen. Subsequently, Potonié (1958) formulated the diagnosis and pointed out that this genus was characterised by elliptical to fusiform outline with longitudinal plicae and a delicate zig-zag line between each pair of plicae (Potonié 1958; Jansonius & Hills 1980). The grooves between plicae and their characteristics have been variously denoted as pseudosulci (Huynh 1975; Bolinder et al. 2016), colpi (Steeves & Barghoorn 1959; Bharadwaj 1963; Zhang & Xi 1983), hyaline lines (Wodehouse 1935; Steeves & Barghoorn 1959; Kedves 1987; Kurmann & Zavada 1994; El-Ghazaly & Rowley 1997) and Z-lines (Krutzsch 1961, 1970; Song 1978, 1999). To avoid confusion, we will consistently use the term pseudosulcus in the present paper (for justification, see Bolinder et al. 2015), also when citing authors that originally used another term.

After the work by Potonié (1958), Krutzsch (1961) demonstrated that the two specimens illustrated by Thiergart (1938) were morphologically dissimilar and that one of the specimens was not of ephedraceaen affinity. He further concluded that *Gnetaceaepollenites* was invalid (Krutzsch 1961). Jansonius (1962) revised this genus to include pollen that is morphologically similar to that of *Ephedra* and *Welwitschia*. De Lima (1979a) summed up the diagnostic characters of *Gnetaceaepollenites* as polyplicate, ellipsoidal to elongate pollen with a few to numerous plicae that run from one tip to the other without fusion and no visible marks.

Bolkhovitina (1953) first described the fossil polyplicate pollen and erected *Ephedripites* and *Welwitschiapites*. Later, Bolkhovitina (1961) renamed that fossil polyplicate pollen as '*Schizaeites*', which was assumed to be related to *Ephedra* (Pocock 1964). After that, Krutzsch (1961) emended *Ephedripites* and gave a detailed description. Later, Pocock (1964) mentioned that *Ephedripites* was of doubtful affinity and he amended *Equisetopollenites*, which was described by Daugherty (1941), to include all the ephedroid pollen, and considered *Ephedripites* as senior synonym. Azéma and Boltenhagen (1974) accepted the validity of *Ephedripites* and *Gnetaceaepollenites*.

Systematic palynology

A total of 30 polyplicate pollen types belonging to three different genera were found in the samples:four *Gnetaceaepollenites*-types, three *Ephedripites*-types

Figure 4. Light micrographs of Eocene ephedroid pollen from the Xining Basin. The sample number and England Finder reference are given for each specimen. **A.** *Steevesipollenites cupuliformis* (PTF02, L35/4). **B.** *Ephedripites* (*E.*) *montanaensis* (PTF02, G41/3). **C.** *Ephedripites* (*E.*) *montanaensis*. (TS-1, K49/4). **D.** *Ephedripites* (*D.*) *eocenipites* (PTF02, S41/2). **E.** *Ephedripites* (*D.*) *fusiformis* (PTF02, M34/4). **F.** *Ephedripites* (*D.*) *megafusiformis* (PTF14, G40/3). **G.** *Ephedripites* (*D.*) *fushunensis* (TS-1, J57/4). **H.** *Ephedripites* (*D.*) *lusaticus* (PTF02, K35/1). **I.** *Steevesipollenites major* (TS-1, Q42/1). **J.** *Steevesipollenites jianxiensis* (PTF02, V35/2). **K.** *Steevesipollenites globosus* (PTF02, T39/3). **L.** *Steevesipollenites globosus* (TS-1, V51/2). **M.** *Steevesipollenites* cf. *S. binodosus* (PTF02, V34/4). **N.** *Ephedripites* (*E.*) *notensis* (PSW02, L34/3). **O.** *Ephedripites* (*D.*) *bernheidensis* (PTF15, W46/1). **P.** *Ephedripites* (*E.*) *lanceolatus* (TS-1, S51/3). **Q.** *Ephedripites* (*E.*) sp. (PTF02, O45/2). **R.** *Ephedripites* (*D.*) *longiformis* (PTF14, L39/2). **S.** *Ephedripites (D.) nanlingensis* (PTF14, T50/4). **T.** *Ephedripites* (*D.*) *megafusiformis* (TS-1, N51/3). **U.** *Ephedripites* (*D.*) *fusiformis* (TS-1, P44/4). **V.** *Ephedripites* (*D.*) *oblongatus* (PTF02, M47/2). **W.** *Ephedripites (D.) cheganica* (PTF02, K37/3). **X.** *Ephedripites* (*D.*) *major* (TS-1, R63/4). **Y.** *Ephedripites (D.) tertiarius* (PTF02, L42/3). **Z.** *Ephedripites (D.) obesus* (TS-1, S47/1). Scale bar – 10 μm.

and one *Steevesipollenites*-type in the Late Cretaceous samples; 17 *Ephedripites*-types and six *Steevesipollenites*-types appear in the Eocene samples; two *Ephedra*-types were found in the Quaternary samples. Table I provides a summary of morphological characteristics and Figures 4–7 include photographic illustrations of key pollen types. The diagnoses and descriptions, here including details of the pseudosulci, are based on our own observation in combination with the description of the original authors (adapted if needed). Dimensions in diagnoses are range values; dimensions in the descriptions are arithmetic means of observed values.

Order Gnetales

Genus Ephedripites *Bolchovitina ex Potonié emend. Krutzsch*

Remarks. — According to the presence or absence of side branches on the pseudosulci, *Ephedripites* is divided into the two subgenera *Ephedripites* and *Distachyapites*, which correspond to the modern pollen types, the ancestral type and the derived type (Bolinder et al. 2016), respectively.

Affinity. — *Ephedra*.

Ephedripites *subgenus* Distachyapites *Krutzsch*

Diagnosis. — Polyplicate pollen with a low number of plicae (approximately 3–8) and a branched pseudosulcus between each pair of plicae; plicae are usually straight or slightly sinuous (Krutzsch 1961).

Ephedripites (Distachyapites) bernheidensis *Krutzsch* (Figure 4O)

1961 *Ephedripites (Distachyapites) bernheidensis*, Krutzsch, p. 25, pl. 2, figs 22–26.
1980 *Ephedripites (Distachyapites) bernheidensis*, Sun and He, p. 91, pl. 18, figs 12, 14.
1999 *Ephedripites (Distachyapites) bernheidensis*, Song, p. 244, pl. 75, figs 17–18.

Diagnosis. — Polyplicate, medium-large sized grain (40–55 μm in long equatorial diameter); peroblate, 6–9 straight or slightly sinuous plicae, poorly defined pseudosulci, *P*/*E* ratio ranges from 0.45 to 0.5.

Description. — Monad, symmetry bilateral, isopolar, peroblate, seven slightly curved plicae fused at the tips, plicae *c*. 1 μm wide, grooves *c*. 8 μm wide, poorly defined pseudosulci with rarely occurring first-order branches.

Dimensions. — Polar axis 23.5 μm; long equatorial diameter 50 μm; *P*/*E* ratio 0.47.

Occurrence. — Shuiwan section, Xining Basin (Eocene).

Remarks. — This species is characterised by its rarely branched pseudosulci and the higher number of plicae relative to other species of *Ephedripites* subgen. *Distachyapites*.

Ephedripites (Distachyapites) cheganica (*Shakhmundes) Ke et Shi* (Figure 4W)

1965 *Ephedra cheganica*, Shakhmundes, p. 221, pl. 2, figs 1–4.
1978 *Ephedripites (Distachyapites) cheganica* (Shakhmundes) Ke et Shi, Song, p. 97, pl. 32, figs 1–3.
1985 *Ephedripites (Distachyapites) cheganica*, Zhu et al., p. 85, pl. 31, fig. 4.
1999 *Ephedripites (Distachyapites) cheganica*, Song, p. 244, pl. 73, figs 9–10.

Diagnosis. — Polyplicate, crenate margin, medium-large sized grain (40–70 μm in long equatorial diameter); peroblate–oblate, 5–7 straight plicae, pseudosulci with well-defined branches, *P*/*E* ratio ranges from 0.4 to 0.6.

Description. — Monad, symmetry bilateral, isopolar, peroblate-oblate; fusiform shaped, five straight plicae fuse at the tips, plicae *c*. 2 μm wide, grooves *c*. 10 μm wide, pseudosulci with long first-order branches. The long first-order branches reach all the way to the plicae and form the crenate margin.

Dimensions. — Polar axis 22 μm, long equatorial diameter 52 μm; *P*/*E* ratio 0.42.

Occurrence. — Shuiwan section, Xining Basin (Eocene).

Remarks. — Shakhmundes (1965) first described this species as having large grains with branched pseudosulci. Krutzsch (1970) considered that *Ephedra cheganica* Shakhmundes was a synonym of *Ephedripites (Distachyapites) eocenipites*. After that, Song (1978) combined *Ephedra cheganica* with similar but larger pollen grains (up to 71 μm in long equatorial diameter) as *Ephedripites (Distachyapites) cheganica* (Shakhmundes) Ke et Shi, and this species is characterised by its crenate margin. *Ephedripites* (*Distachyapites*) *cheganica* is different *from E. (D.) eocenipites* in its acute tips and the size of *E. (D.)*

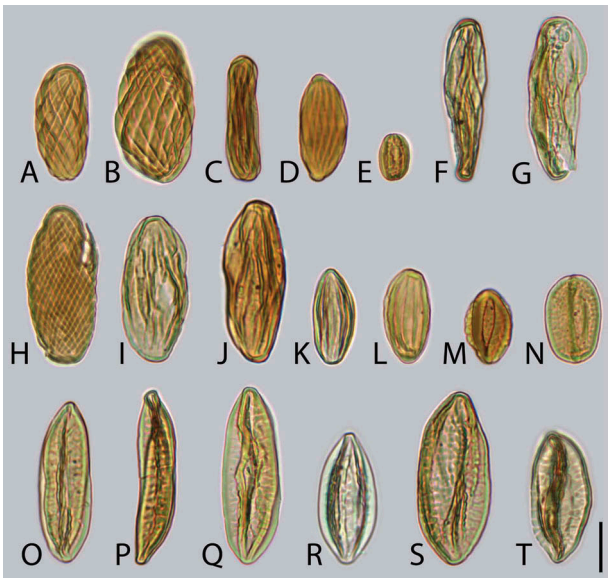

Figure 5. Light micrographs of fossil ephedroid pollen selected by single grain technique in the study area. The sample number is given for each specimen. **A.** *Gnetaceaepollenites barghoornii* (O2X351). **B.** *Gnetaceaepollenites* sp. 1 (O2X351). **C.** *Gnetaceaepollenites* sp. 2 (O2X351). **D.** *Steevesipollenites communis* (PSW03). **E.** *Gnetaceaepollenites* sp. 3 (O2X351). **F.** *Steevesipollenites cupuliformis* (PSW41). **G.** *Ephedripites* (*E.*) *montanaensis* (PSW41). **H.** *Ephedripites* (*S.*) *retiformis* (O2X351). **I.** *Ephedripites* (*E.*) *lanceolatus* (PSW34). **J.** *Ephedripites* (*E.*) *lanceolatus* (PSW41). **K.** *Ephedra* sp. 2 (Q437.25). **L.** *Ephedripites* (*E.*) *notensis* (O2X351). **M.** *Ephedripites* (*D.*) *fushunensis* (O2X535). **N.** *Ephedripites* (*D.*) *lusaticus* (PSW41). **O.** *Ephedripites* (*D.*) *fusiformis* (PSW03). **P.** *Ephedripites* (*D.*) *longiformis* (PSW34). **Q.** *Ephedripites* (*D.*) *megafusiformis* (PTF14). **R.** *Ephedra* sp. 1 (Q39.75). **S.** *Ephedripites* (*D.*) *eocenipites* (PSW34). **T.** *Ephedripites* (*D.*) *claricristatus* (PSW34). Scale bar – 20 μm.

cheganica is much bigger than that of *E. (D.) fushunensis*

Ephedripites (Distachyapites) claricristatus (*Shakmundes*) *Krutzsch*
(Figures 5T, 6T, 7A)

1965 *Ephedripites claricristata*, Shakhmundes, p. 226, pl. 4, figs 4–6.
1970 *Ephedripites (Distachyapites) claricristatus* (Shakhmundes), Krutzsch, p. 158, pl. 45, figs 1–31.
1999 *Ephedripites (Distachyapites) claricristatus*, Song, p. 244, pl. 73, figs 7–8.

Diagnosis. — Polyplicate, medium sized grain (33–50 μm in long equatorial diameter); peroblate-oblate, 4–7 straight or slightly sinuous plicae, pseudosulci with prominent branches, *P*/*E* ratio ranges from 0.4 to 0.6.

Description. — Monad, symmetry bilateral, isopolar, peroblate-oblate; four slightly sinuous plicae fuse at the tips, plicae *c.* 2 μm wide, grooves *c.* 6.5 μm wide, significantly branched pseudosulci with first- and second-order branches, and the branching not always occurring at the angles formed by the undulations of the pseudosulci.

Dimensions. — Polar axis 21 μm, long equatorial diameter 47 μm; *P*/*E* ratio 0.44.

Occurrence. — Shuiwan section, Xining Basin (Eocene).

Remarks. — *Ephedripites (Distachyapites) fusiformis*, *E. (D.) lusaticus*, *E. (D.) claricristatus* and *E. (D.) eocenipites* all are similar to each other. Krutzsch (1970) considers that the most practical criterion for separating the species is the *P*/*E* ratio, as follows: *E. (D.) fusiformis* is more slender (0.3–0.4), the *P*/*E* ratio of *E. (D.) claricristatus* (0.4–0.6) is the same as *E. (D.) eocenipites*, however, the latter one is larger, *E. (D.) lusaticus* is smaller and stockier (0.6–0.7).

Ephedripites (Distachyapites) eocenipites *(Wodehouse) Krutzsch*
(Figures 4D, 5S, 6S, 7B, C)

1933 *Ephedra eocenpites*, Wodehouse, p. 495, fig. 20.
1958 *Gnetaceaepollenites eocenipites* (Wodehouse 1933), Potonié.
1961 *Ephedripites (Distachyapites) eocenipites* (Wodehouse), Krutzsch, p. 27, pl. 3, fig. 41.
1965 *Ephedra eocenica* Schakhmundes, p. 219, text-figs 2–3.
1999 *Ephedripites (Distachyapites) eocenipites*, Song, p. 245, pl. 72, figs 7–9.

Diagnosis. — Polyplicate, large sized grain (50–75 μm in long equatorial diameter), peroblate–oblate, 5–7 slightly sinuous or straight plicae, typically branched pseudosulci, *P*/*E* ratio ranges from 0.4 to 0.6.

Description. — Monad, symmetry bilateral, isopolar, peroblate, seven plicae with angular shape fuse at the tips while one plica vanishes in the groove, plicae *c.* 2 μm width, grooves *c.* 10 μm wide, typically branched pseudosulci with long first-order branches.

Dimensions. — Polar axis 28.2 μm, long equatorial diameter 66.4 μm; *P*/*E* ratio 0.4.

Occurrence. — Shuiwan section, Xining Basin (Eocene).

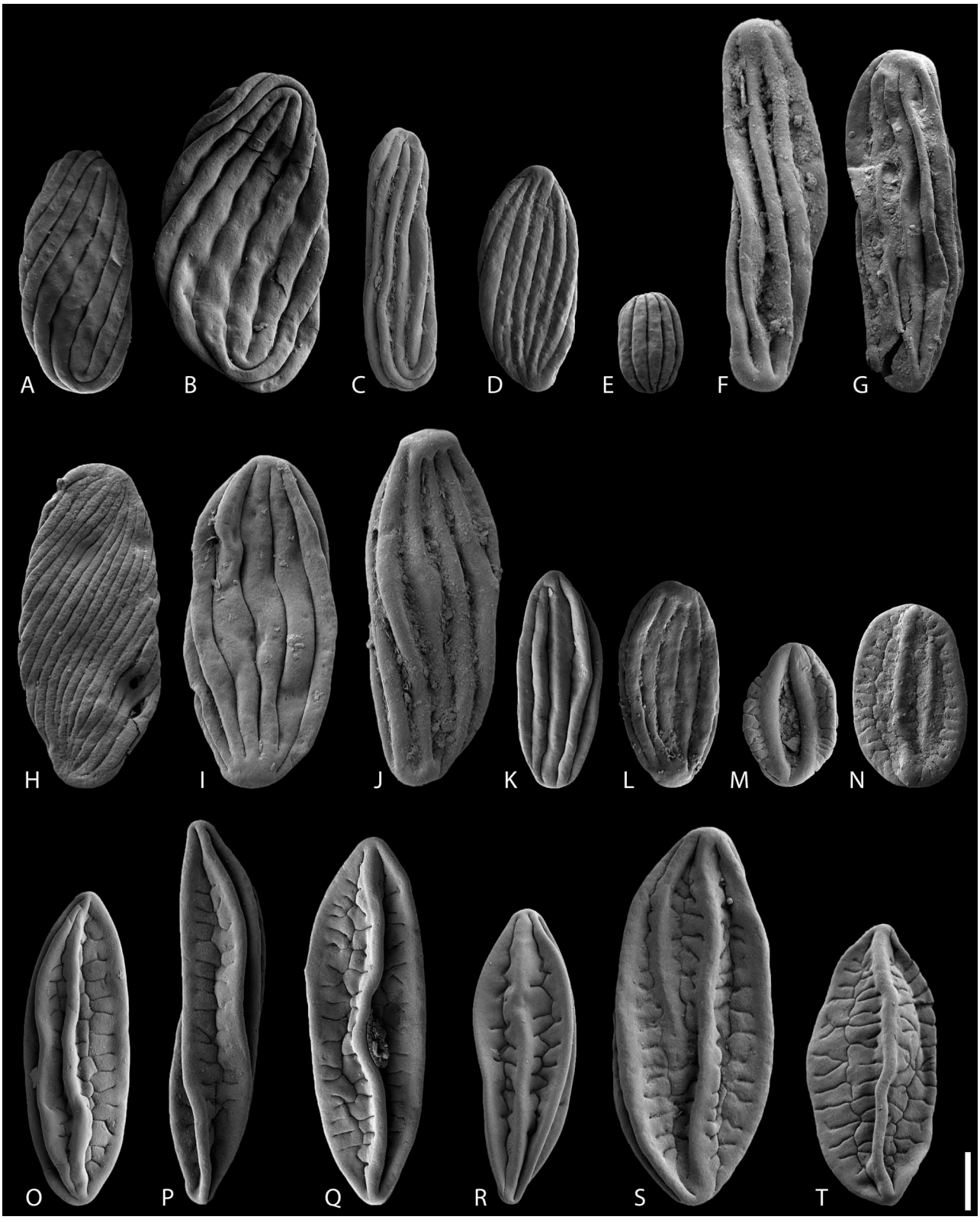

Figure 6. Scanning electron micrographs of the same fossil pollen grains as in Figure 5. The sample number is given for each specimen. **A.** *Gnetaceaepollenites barghoornii* (O2X351). **B.** *Gnetaceaepollenites* sp.1 (O2X351). **C.** *Gnetaceaepollenites* sp. 2 (O2X351). **D.** *Steevesipollenites communis* (PSW03). **E.** *Gnetaceaepollenites* sp. 3 (O2X351). **F.** *Steevesipollenites cupuliformis* (PSW41). **G.** *Ephedripites* (*E.*) *montanaensis* (PSW41). **H.** *Ephedripites* (*S.*) *retiformis* (O2X351). **I.** *Ephedripites* (*E.*) *lanceolatus* (PSW34). **J.** *Ephedripites* (*E.*) *lanceolatus* (PSW41). **K.** *Ephedra* sp. 2 (Q437.25). **L.** *Ephedripites* (*E.*) *notensis* (O2X351). **M.** *Ephedripites* (*D.*) *fushunensis* (O2X535). **N.** *Ephedripites* (*D.*) *lusaticus* (PSW41). **O.** *Ephedripites* (*D.*) *fusiformis* (PSW03). **P.** *Ephedripites* (*D.*) *longiformis* (PSW34). **Q.** *Ephedripites* (*D.*) *megafusiformis* (PTF14). **R.** *Ephedra* sp. 1 (Q39.75). **S.** *Ephedripites* (*D.*) *eocenipites* (PSW34). **T.** *Ephedripites* (*D.*) *claricristatus* (PSW34). Scale bar – 10 μm.

Remarks. — The vanished plica is common in *Ephedripites (Distachyapites) eocenipites*. It has also been observed in modern *Ephedra* pollen and is more likely caused by abnormal growth. It does not seem to be a diagnostic character of this species.

Ephedripites (Distachyapites) fushunensis *Sung et Tsao*
(Figures 4G, 5M, 6M, 7D)

1980 *Ephedripites (Distachyapites) fushunensis*, Sung and Tsao, p. 4, pl. 2, figs 18–19.
1980 *Ephedripites (Distachyapites) palaeocenicus*, Sun and He, p. 94, pl. 17, figs 17–22.
1999 *Ephedripites (Distachyapites) fushunensis*, Song, p. 246, pl. 73, figs 1–3.

Diagnosis. — Polyplicate, medium sized (20–40 μm in long equatorial diameter), oblate, crenate margin, 3–5 stout plicae that fuse at the tips forming a fusiform or a circular shape.

Description. — Monad, symmetry bilateral, isopolar, oblate; five wide plicae fuse at the tips, the width of plicae is *c.* 4 μm, the plica articulates with the adjacent plica forming a fusiform or a circular shape, groove 4.5 μm wide, pseudosulci with long first-order branches, the first-order branches usually bifurcate or trifurcate forming second- and third-order branches; the branches reach all the way to the plicae and form the crenate margin.

Dimensions. — Polar axis 22 μm, long equatorial diameter 35 μm; *P*/*E* ratio 0.65.

Occurrence. — Shuiwan section, Xining Basin (Eocene).

Remarks. — *Ephedripites (Distachyapites) palaeocenicus* Sun et He and *E. (D.) fushunensis* are of the same size; both of them have wider plicae and crenate margins. Sung and Tsao (1980) first described *E. (D.) fushunensis* without defining a holotype. Sun and He (1980) named it *E. (D.) palaeocenicus*. We here consider *E. (D.) palaeocenicus* a junior synonym of *E. (D.) fushunensis*.

Ephedripites (Distachyapites) fusiformis *(Shakhmundes) Krutzsch*
(Figures 4E, U, 5O, 6O, 7E)

1961 *Ephedripites (Distachyapites)? trinata* (Zaklinskaya), Krutzsch, p. 21.
1965 *Ephedripites fusiformis*, Shakhmundes, p. 222, pl. 3, figs 1–6.
1970 *Ephedripites (Distachyapites) fusiformis* (Shakhmundes), Krutzsch, p. 160, pl. 46, figs 1–31.
1980 *Ephedripites (Distachyapites) zigzagus*, Sun and He, p. 94, pl. 19, figs 3–7
1999 *Ephedripites (Distachyapites) fusiformis*, Song, p. 246, pl. 71, figs 16, 17, 22, 23

Diagnosis. — Polyplicate, medium-large sized grain (35–60 μm in long equatorial diameter); peroblate, a low number of straight or slightly spiral plicae (approximately 4–8), typically branched pseudosulci, *P*/*E* ratio range from 0.3 to 0.4.

Description. — Monad, symmetry bilateral, isopolar, peroblate; fusiform pollen with six straight to slightly sinuous plicae that fuse at the tips, the width of plicae is *c.* 2 μm, grooves *c.* 7 μm wide, pseudosulci with long first-order branches, and branching occurs at the angles formed by the undulations of the pseudosulci. Most of the first-order branches are straight, and few bifurcate at the end forming second-order branches.

Dimensions. — Polar axis 20 μm, long equatorial diameter 57 μm; *P*/*E* ratio 0.35.

Occurrence. — Shuiwan section, Xining Basin (Eocene).

Remarks. — Krutzsch (1961) mentioned the species *Ephedripites (Distachyapites)? trinata* (Zakl.) with uncertainty. The only difference between *E. (D.) trinata* and *E. (D.) fusiformis* is the number of plicae. It seems like *E. (D.) trinata* has three plicae under LM; however, we have confirmed that it has at least four plicae using SEM. As such, *E. (D.) trinata* is a synonym of *E. (D.) fusiformis*.

Ephedripites (Distachyapites) longiformis *Sun et He*
(Figures 4R, 5P, 6P, 7F)

1980 *Ephedripites (Distachyapites) longiformis*, Sun and He, p. 95, pl. 20, fig. 15.
1991 *Ephedripites (Distachyapites) longiformis*, Zhang and Zhan, p. 183, pl. 59, figs 13–14, pl. 60, figs 27–30.
1999 *Ephedripites (Distachyapites) longiformis*, Song, p. 247, pl. 73, figs 16–17.

Diagnosis. — Polyplicate, large sized grain (50–80 μm in long equatorial diameter); peroblate, this species is characterised by its elongate shape, a low number of slightly spiral plicae (approximately 4–6), typically branched pseudosulci, *P*/*E* ratio < 0.25.

Description. — Monad, symmetry bilateral, isopolar, peroblate; five slightly spiral plicae fuse at the tips, plicae *c.* 2 μm wide, grooves *c.* 7 μm wide, typically branched pseudosulci with first-order branches, the branching occurs at the angles formed by the undulations of the pseudosulci, most of the first-order branches are straight.

Dimensions. — Polar axis 13 μm, long equatorial diameter 65 μm; *P*/*E* ratio 0.2.

Occurrence. — Shuiwan section, Xining Basin (Eocene).

Remarks. — This species differs from *Ephedripites (Distachyapites) fusiformis* in having a smaller *P*/*E* ratio and elongate shape.

Ephedripites (Distachyapites) lusaticus *Krutzsch*
(Figures 4H, 5N, 6N, 7G)

1961 *Ephedripites (Distachyapites) lusaticus*, Krutzsch, p. 26, pl. 6, figs 120–128.
1970 *Ephedripites (Distachyapites) lusaticus*, Krutzsch, p. 162, pl. 47, figs 1–21.
1980 *Ephedripites (Distachyapites) lusaticus*, Sun et al., p. 95, pl. 20, fig. 28.
1999 *Ephedripites (Distachyapites) lusaticus*, Song, p. 247, pl. 74, fig. 5.

Diagnosis. — Polyplicate, medium sized grain (28–44 μm in long equatorial diameter), oblate, 4–8 plicae with small protuberance in the tip area, typically branched pseudosulci, *P*/*E* ratio range from 0.6 to 0.7.

Description. — Monad, symmetry bilateral, isopolar, oblate; five plicae, about 2 μm width, plicae with acute ends fused in the tip area to form a small protuberance; there is one plicae with two ends vanishing in the grooves that only appears in the middle part of the grain; the width of grooves is *c.* 6.5 μm, pseudosulci with long first-order branches; the branching occurs at the angles formed by the undulations of the pseudosulcus, some of the first-order branches bifurcate at the end forming second-order branches.

Dimensions. — Polar axis 22 μm, long equatorial diameter 37 μm; *P*/*E* ratio 0.6.

Occurrence. — Shuiwan section, Xining Basin (Eocene).

Remarks. — This species has a general similarity to *Ephedripites (Distachyapites) fushunensis*, but the plicae of *E. (D.) fushunensis* are much more pronounced than those of *E. (D.) lusaticus*. The branching pattern of the pseudosulci is also more complex in *E. (D.) fushunensis* than in *E. (D.) lusaticus*.

Ephedripites (Distachyapites) major *Ke et Shi*
(Figure 4X)

1978 *Ephedripites (Distachyapites) major* Ke et Shi, Song, p. 99, pl. 31, figs 5–8, 10.
1991 *Ephedripites (Distachyapites) major*, Zhang et Zhan, p. 184, pl. 59, figs 22–23.
1999 *Ephedripites (Distachyapites) major*, Song, p. 247, pl. 72, figs 13–15.

Diagnosis. — Polyplicate, large sized grain (> 80 μm in long equatorial diameter); peroblate, 4–8 plicae, typically branched pseudosulci, *P*/*E* ratio range from 0.3 to 0.5.

Description. — Monad, symmetry bilateral, isopolar, peroblate; eight slightly sinuous plicae which fuse at the tips. The width of plicae is *c.* 1 μm, grooves *c.* 4.5 μm wide, and typically branched pseudosulci.

Dimensions. — Polar axis 26 μm, long equatorial diameter 80 μm; *P*/*E* ratio 0.33.

Occurrence. — Shuiwan section, Xining Basin (Eocene).

Remarks. — This species differs from *Ephedripites (Distachyapites)* sp. in being larger (> 80 μm in equatorial diameter).

Ephedripites (Distachyapites) megafusiformis *Ke et Shi*
(Figures 4F, T, 5Q, 6Q, 7H)

1978 *Ephedripites (Distachyapites) megafusiformis* Ke et Shi, Song, p. 99, pl. 31, figs 5–8, 10.
1985 *Ephedripites (Distachyapites) parafusiformis*, Zhu and Wu, p. 91, pl. 32, figs 24–26.
1991 *Ephedripites (Distachyapites) megatrinatus*, Zhang and Zhan, p. 184, pl. 58, figs 20–21, 31.
1999 *Ephedripites (Distachyapites) megafusiformis*, Song, p. 247, pl. 72, figs 4–6.

Diagnosis. — Polyplicate, large sized grain (60–80 μm in long equatorial diameter); peroblate, a low number of straight or slightly sinuous plicae (4–6), pseudosulci with first-order branches, *P*/*E* ratio range from 0.27 to 0.4.

Description. — Monad, symmetry bilateral, isopolar, peroblate; five slightly sinuous plicae fuse at the tips, the width of the plicae is *c.* 1.7 μm, grooves *c.* 9 μm

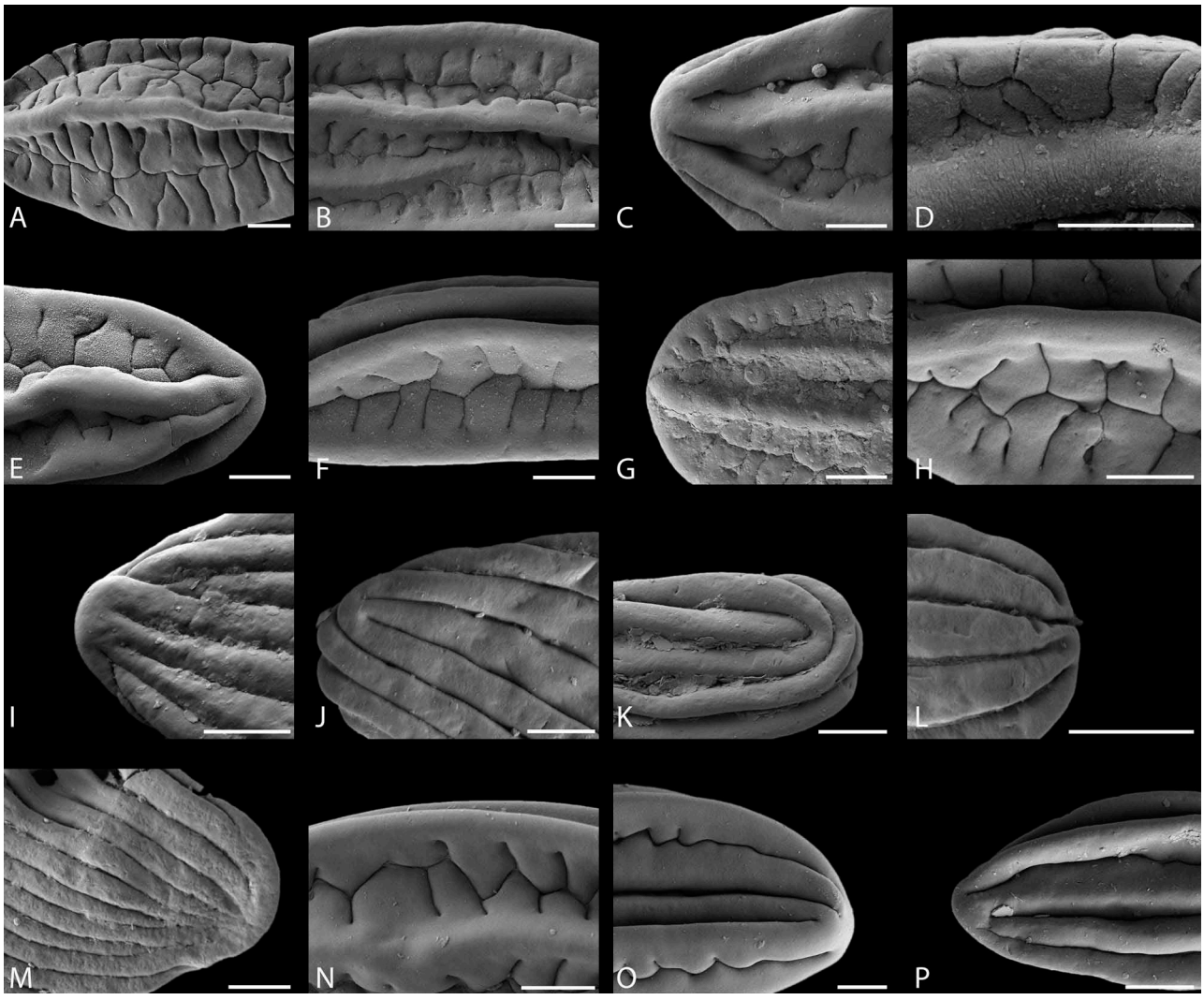

Figure 7. Details of plicae and branched pseudosulci of selected species, scanning electron micrographs. The sample number is given for each specimen. **A.** Third order of branching, *Ephedripites* (*D.*) *claricristatus* (PSW34). **B.** First order of branching and vanished rib, *Ephedripites* (*D.*) *eocenipites* (PSW34). **C.** First order of branching and fused plicae, *Ephedripites* (*D.*) *eocenipites* (PSW34). **D.** Second order of branching and wide rib, *Ephedripites* (*D.*) *fushunensis* (O2X535). **E.** Second order of branching and fused plicae, *Ephedripites* (*D.*) *fusiformis* (PSW03). **F.** First order of branching, *Ephedripites* (*D.*) *longiformis* (PSW34). **G.** Second order of branching and small protuberance, *Ephedripites* (*D.*) *lusaticus* (PSW41). **H.** Second order of branching, *Ephedripites* (*D.*) *megafusiformis* (PTF14). **I.** Thick exine, *Steevesipollenites communis* (PSW03). **J.** Partly fused plicae, *Gnetaceaepollenites barghoornii* (O2X351). **K.** None-fused plicae, *Gnetaceaepollenites* sp.2 (O2X351). **L.** Partly fused plicae, *Gnetaceaepollenites* sp.3 (O2X351). **M.** Fused plicae, *Ephedripites* (*S.*) *retiformis* (O2X351). **N.** First order of branching, *Ephedra sp.*1 (Q39.75). **O.** First order of branching, *Ephedra sp.*2 (Q39.75). **P.** Unbranched pseudosulci, *Ephedra* sp. 2 (Q437.25). Scale bars – 5 μm.

wide. The pseudosulci have first-order branches, and branching occurs at the angles formed by the undulations of the pseudosulci; few first-order branches bifurcate at the end and form second-order branches.

Dimensions. — Polar axis 20 μm, long equatorial diameter 68 μm; *P*/*E* ratio 0.3.

Occurrence. — Shuiwan section, Xining Basin (Eocene).

Remarks. — This species differs from *Ephedripites (Distachyapites) fusiformis* only in being larger than the latter species. Zhu et al. (1985) named it *E. (D.) parafusiformis* because it has a slightly different *P*/*E* ratio (0.41); Zhang and Zhan (1991) named it *E. (D.) megatrinatus* after the number of plicae (three plicae); both of these two species have the same size and same branched pseudosulci as *E. (D.) megafusiformis*. We consider *E. (D.) megafusiformis* the valid name and *E. (D.) parafusiformis* and *E. (D.) megatrinatus* as senior synonyms.

Ephedripites (Distachyapites) nanlingensis *Sun et He* (Figure 4S)

1980 *Ephedripites (Distachyapites) nanlingensis*, Sun and He, p. 92, pl. 19, figs 12–16.
1991 *Ephedripites (Distachyapites) nanlingensis*, Zhang and Zhan, p. 185, pl. 59, figs 1–4.
1999 *Ephedripites (Distachyapites) nanlingensis*, Song, p. 249, pl. 72, figs 1–3.

Diagnosis. — Polyplicate, medium-large sized grain (40–70 μm in long equatorial diameter); peroblate, a low number of straight or slightly spiral plicae (5–7), typically branched pseudosulci, *P*/*E* ratio range from 0.33 to 0.4.

Description. — Monad, symmetry bilateral, isopolar, peroblate; five slightly spiral plicae fuse at the tips, the width of plicae is *c*. 2 μm, grooves *c*. 7 μm wide, pseudosulci with first-order branches, most of the first-order branches bifurcate at the end and form second-order branches.

Dimensions. — Polar axis 22 μm, long equatorial diameter 65 μm; *P*/*E* ratio 0.33.

Occurrence. — Shuiwan section, Xining Basin (Eocene).

Remarks. — This species differs from *Ephedripites (Distachyapites) fusiformis* only in having relatively rounded tips.

Ephedripites (Distachyapites) obesus *Ke et Shi* (Figure 4Z)

1978 *Ephedripites (Distachyapites) obesus*, Ke and Shi, Song, p. 99, pl. 30, fig. 12.
1991 *Ephedripites (Distachyapites) obesus*, Zhang and Zhan, p. 185, pl. 58, fig. 26.
1999 *Ephedripites (Distachyapites) obesus*, Song, p. 249, pl. 73, figs 21–22.

Diagnosis. — Polyplicate, medium-large sized grain (40–57 μm in long equatorial diameter); suboblate-subspheroidal, 4–6 straight or slightly sinuous plicae, pseudosulci with significantly branches, *P*/*E* ratio range from 0.7 to 0.9.

Description. — Monad, symmetry bilateral, isopolar, suboblate-subspheroidal; six slightly sinuous plicae fuse at the tips, plicae *c*. 1.5 μm wide, pseudosulci with long first-order branches, most of the first-order branches bifurcate at the end and form second-order branches.

Dimensions. — Polar axis 31 μm, long equatorial diameter 44 μm; *P*/*E* ratio 0.70.

Occurrence. — Shuiwan section, Xining Basin (Eocene).

Remarks. — The plicae are strongly waved in some grains of this species. Such strongly waved plicae are common in modern *Ephedra* pollen grains that have been treated with ethanol; thus, we hypothesise that the strongly waved plicae may be an artificial effect of treatment with ethanol during processing of the samples.

Ephedripites (Distachyapites) oblongatus *Ke et Shi* (Figure 4V)

1978 *Ephedripites (Distachyapites) oblongatus*, Ke and Shi, p. 100, pl. 30, figs 13–14.
Song, pl. 32, figs 4–8.

1991 *Ephedripites (Distachyapites) oblongatus*, Zhang and Zhan, p. 185, pl. 58, figs 9–10.
1999 *Ephedripites (Distachyapites) oblongatus*, Song, p. 250, pl. 74, figs 20–22.

Diagnosis. — Polyplicate, medium-large sized grain (40–55 μm in long equatorial diameter); oblate-suboblate, 4–7 straight or slightly sinuous plicae, typically branched pseudosulci, *P*/*E* ratio range from 0.6 to 0.8.

Description. — Monad, symmetry bilateral, isopolar, oblate-suboblate; four slightly sinuous plicae fuse at the tips, plicae *c*. 1 μm wide, grooves *c*. 10 μm wide, pseudosulci with long first-order branches, the branching occurs at the angles formed by the undulations of the pseudosulci.

Dimensions. — Polar axis 28 μm, long equatorial diameter 45 μm; *P*/*E* ratio 0.62.

Occurrence. — Shuiwan section, Xining Basin (Eocene).

Remarks. — The definition of species *Ephedripites (Distachyapites) oblongatus* is very loose (similar to some pollen grains of *E. [D.] claricristatus* and *E. [D.] eocenipites*, but differs from the holotype), and the crenate margin of this species is very similar to that of *E. (D.) cheganica*. However, the *P*/*E* ratio of *E. (D.) oblongatus* is larger than that of *E. (D.) cheganica*.

Ephedripites (Distachyapites) tertiarius *Krutzsch* (Figure 4Y)

1970 *Ephedripites (Distachyapites) tertiarius*, Krutzsch, p. 156, pl. 44, figs 1–21.

1980 *Ephedripites (Distachyapites) tertiarius*, Sun and He, p. 90, pl. 17, fig. 11.
1999 *Ephedripites (Distachyapites) tertiarius*, Song, p. 252, pl. 74, figs 13–15.

Diagnosis. — Polyplicate, medium-large sized grain (45–55 μm in long equatorial diameter), peroblate, 4–8 slightly sinuous or straight plicae, typically branched pseudosulci, *P*/*E* ratio range from 0.4 to 0.5.

Description. — Monad, symmetry bilateral, isopolar, peroblate, five slightly sinuous plicae fuse at the tips, plicae *c*. 2 μm wide, grooves *c*. 11 μm wide, pseudosulci with long first- and second-order branches.

Dimensions. — Polar axis 20 μm, long equatorial diameter 47 μm; *P*/*E* ratio 0.42.

Occurrence. — Shuiwan section, Xining Basin (Eocene).

Remarks. — Frederiksen (1973) considered that *Ephedripites (Distachyapites) tertiarius* is a synonym to *E. (D.) claricristatus*, but we consider that *E. (D.) tertiarius* differs from *E. (D.) claricristatus* because the latter tends to have relatively more rounded ends. This species is very similar to *E. (D.) eocenipites*, whereas *E. (D.) tertiarius* is distinguished by the smaller size and the generally slimmer shape.

Ephedra *sp. 1*
(Figures 5R, 6R, 7N)

Description. — Polyplicate, medium-large sized grain (40–60 μm in long equatorial diameter), peroblate, 4–8 slightly sinuous or straight plicae, typically branched pseudosulci, *P*/*E* ratio range from 0.25 to 0.4. Monad, symmetry bilateral, isopolar, peroblate, six slightly sinuous plicae fuse at the tips, plicae *c*. 2 μm wide, grooves *c*. 5 μm wide, pseudosulci with short straight first-order branches.

Dimensions. — Polar axis 18 μm, long equatorial diameter 53 μm, *P*/*E* ratio 0.33.

Occurrence. — SG-1 core, Qaidam Basin (Quaternary).

Ephedra *sp. 2*
(Figures 5K, 6K, 7O, 7P)

Description. — Polyplicate, medium-large sized grain (35–65 μm in long equatorial diameter), peroblate, 8–14 slightly sinuous or straight plicae, pseudosulci with short first-order branches or without first-order branches, *P*/*E* ratio range from 0.3 to 0.4. Monad, symmetry bilateral, isopolar, peroblate, 10 slightly sinuous plicae fuse at the tips, plicae *c*. 3 μm wide, grooves *c*. 1.5 μm wide, pseudosulci without first-order branches.

Dimensions. — Polar axis 13 μm, long equatorial diameter 35 μm; *P*/*E* ratio 0.37.

Occurrence. — SG-1 core, Qaidam Basin (Quaternary).

Remarks. — The two types of Neogene *Ephedra* pollen grains that were found in the Qaidam Basin may belong to the following high elevation species, namely *E. intermedia, E. gerardiana, E. przewalskii* or *E. minuta*. *Ephedra* sp. 1 has pollen grains with a low number of plicae (approximately 4–8) and the pseudosulci between the plicae have obvious first-order branches. This species may be conspecific with *E. intermedia* or *E. gerardiana*, which often has a clearly branched sulcus. *Ephedra* sp. 2 has pollen grains with approximately 8–14 plicae and the narrow valleys between the plicae show unclear pseudosulci, sometimes with short first-order branches. This species may be conspecific with *E. przewalskii* or *E. minuta*, which often have unbranched pseudosulci.

Ephedripites *subgenus* Ephedripites *Krutzsch*

Diagnosis. — Polyplicate pollen with numerous plicae (8–20), pseudosulci between the plicae without first-order branches.

Ephedripites (Ephedripites) lanceolatus *Zhu et Wu*
(Figures 4P, 5I, J, 6I, J)

1985 *Ephedripites (Ephedripites) lanceolatus*, Zhu and Wu, p. 96, pl. 34, figs 23–25.
1999 *Ephedripites (Ephedripites) lanceolatus*, Song, p. 255, pl. 70, figs 15–17.

Diagnosis. — Polyplicate, large sized grain (50–65 μm in long equatorial diameter), peroblate, elliptical outline, 8–14 longitudinal plicae, plicae *c*. 3–4.5 μm wide, *P*/*E* ratio range from 0.3 to 0.5.

Description. — Monad, symmetry bilateral, isopolar, peroblate, outline elliptical, 12 slightly sinuous plicae fuse at the tips, plicae *c*. 4 μm wide, grooves *c*. 1 μm wide, unbranched pseudosulci.

Dimensions. — Polar axis 23 μm, long equatorial diameter 55 μm; *P*/*E* ratio 0.41.

Occurrence. — East Xining, Tiefo, and Shuiwan sections, Xining Basin (Late Cretaceous–middle to late Eocene).

Remarks. — This species is characterised by flat and broad plicae observed in transverse section, but the width of the plicae is less than that of *Ephedripites (Ephedripites) strigatus* Brenner.

Ephedripites (Ephedripites) montanaensis *Brenner*
(Figures 4B, C, 5G, 6G)

1968 *Ephedripites (Ephedripites) montanaensis*, Brenner, p. 362, pl. 6, fig. 8.
1980 *Ephedripites (Ephedripites) montanaensis*, Sun and He, p. 98, pl. 20, figs 8, 13.
1999 *Ephedripites (Ephedripites) montanaensis*, Song, p. 257, pl. 71, figs 9–10.

Diagnosis. — Polyplicate, large sized grain (50–67 μm in long equatorial diameter), peroblate, elongated outline, rounded ends, 10–18 slight inclined plicae, plicae *c.* 1–2 μm width, *P*/*E* ratio range from 0.28 to 0.33.

Description. — Monad, symmetry bilateral, isopolar, peroblate, elongated outline, sub-truncate ends, 12 longitudinal narrow plicae fuse at the tips, plicae *c.* 1.5 μm wide, 3 μm high, grooves *c.* 1 μm wide, unbranched pseudosulci.

Dimensions. — Polar axis 20 μm, long equatorial diameter 62 μm; *P*/*E* ratio 0.32.

Occurrence. — East Xining, Tiefo, and Shuiwan sections, Xining Basin (Late Cretaceous–middle to late Eocene).

Ephedripites (Ephedripites) notensis *(Cookson) Krutzsch*
(Figures 4N, 5L, 6L)

1957 *Ephedripites notensis*, Cookson, p. 45, pl. 9, figs 6–10.
1961 *Ephedripites (Ephedripites) notensis* (Cookson), Krutzsch, p. 20.
1991 *Ephedripites (Ephedripites) notensis*, Zhang and Zhan, p. 188, pl. 31, fig. 33, pl. 60, figs 16, 25–26.
1999 *Ephedripites (Ephedripites) notensis*, Song, p. 258, pl. 69, figs 21–22.

Diagnosis. — Polyplicate, medium sized grain (25–50 μm in long equatorial diameter), peroblate, outline elliptical, 10–15 longitudinal plicae, plicae *c.* 3 μm wide, *P*/*E* ratio range from 0.45 to 0.56.

Description. — Monad, symmetry bilateral, isopolar, perprolate, outline elliptical, oval ends, 12 longitudinal flat plicae fuse at the poles, plicae *c.* 3 μm wide, grooves *c.* 0.5 μm wide, no branched pseudosulci.

Dimensions. — Polar axis 17 μm, long equatorial diameter 36 μm; *P*/*E* ratio 0.47.

Occurrence. — East Xining, Tiefo, and Shuiwan sections, Xining Basin (Late Cretaceous–middle to late Eocene).

Ephedripites *subgenus* Spiralipites *Krutzsch*

Diagnosis. — Polyplicate pollen with numerous rotated plicae with unbranched pseudosulci and mostly found in the Upper Cretaceous.

Ephedripites (Spiralipites) retiformis *Gao et Zhao comb. nov.*
(Figures 5H, 6H, 7M)

1976 *Schizaeoisporites retiformis*, Gao and Zhao, p. 34, pl. 6, figs 3–8.
2002 *Ephedripites* sp., Yi and Batten, p. 697, fig. 7P, Q.

Diagnosis. — Polyplicate, large sized grain (57.5 μm in long equatorial diameter), peroblate, outline elliptical, 25–30 rotated plicae, plicae *c.* 1.5 μm wide, unbranched pseudosulci, *P*/*E* ratio *c.* 0.45.

Specimen. — O2X 351–1

Description. — Monad, symmetry bilateral, isopolar, peroblate, outline elliptical, 25 spirally rotated plicae (flat in transverse section) and with narrow ends that fuse at the tips, forming a 'checkered' pattern under LM; some plicae vanished or joined another plica near the tip area, plicae *c.* 1.5 μm wide, grooves *c.* 0.2 μm wide, unbranched pseudosulci.

Dimensions. — Polar axis 25.7 μm, long equatorial diameter 57.5 μm; *P*/*E* ratio 0.45.

Occurrence. — East Xining section, Xining Basin (Late Cretaceous).

Remarks. — Some species of *Schizaeoisporites* and *Ephedripites* are morphologically similar and can easily be mixed up, especially when the monolete mark of the former is unclear. Song (1999) use the

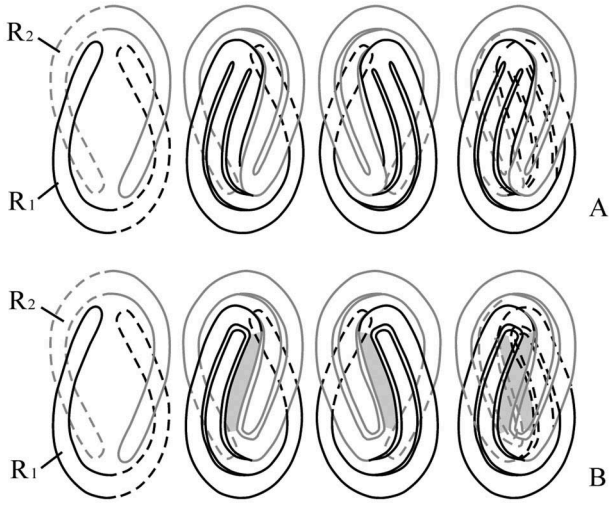

Figure 8. The plicae pattern of *Gnetaceaepollenites*. **A.** The plicae pattern for *Gnetaceaepollenites barghoornii* and *Gnetaceaepollenites* sp. 1. The horseshoe-shaped plicae arranged in two sets R1, R2. **B.** The plicae pattern for *Gnetaceaepollenites* sp. 2. The plicae are arranged in two sets R1 and R2, and are sharing one longitudinal plica (marked with shadow parts).

inclined and none fused plicae to differentiate *Schizaeoisporites* from *Ephedripites*. For this species, although there are numerous inclined plicae forming a 'checkered' pattern, there are no visible laesurae and the plicae fused at the poles. We consider it as *Ephedripites (Schizaeoisporites) retiformis; E. (S.) praeclarus* (Khl.) Krutzsch is larger (57–80 μm in long equatorial diameter) and the plicae (*c.* 3.5 μm) are wider than those of *E. (S.) retiformis*.

Genus Gnetaceaepollenites *Thiergart emend. Jansonius*

Diagnosis. — Polyplicate; ellipsoidal to elongated pollen with a few to numerous plicae; plicae run along the equator plane without fusion at the tips, no visible laesurae.

Gnetaceaepollenites barghoornii *(Pocock) De Lima*
(Figures 5A, 6A, 7J)

1964 *Equisetosporites barghoornii*, Pocock, p. 149, pl. 1, fig. 21.
1976 *Schizaeoisporites laevigataeformis* (Bolchovitina), Gao et Zhao, p. 34, pl. 5, figs 13–16.
1980 *Gnetaceaepollenites barghoornii* (Pocock), Lima, p. 35, pl. 3, fig. 12.

Diagnosis. — Polyplicate, medium sized grain (30–50 μm in long equatorial diameter); peroblate, 10–14 inclined and partly fused plicae, and the plicae arranged in two sets on the opposite sides of grain forming the pattern A (Figure 8A). *P*/*E* ratio range from 0.4 to 0.5.

Description. — Monad, symmetry bilateral, isopolar, peroblate; plicae on one side are oblique to those on the other side, forming a 'checkered' pattern. Five long, horseshoe-shaped, *c.* 2–3 μm wide plicae divided into two sets (R1 and R2) of two or three long plicae each. The plicae start near one tip and cross over the other tip to the opposite side of the grain, ending nearly opposite their point of origin; both ends of the two set of plicae are fused.

Dimensions. — Polar axis 20 μm, long equatorial diameter 42 μm; *P*/*E* ratio 0.47.

Occurrence. — East Xining section, Xining Basin (Late Cretaceous).

Remarks. — The numbers of plicae for each set varies from two to four. Besides the long plicae, there are short plicae that do not cross over the other tip but vanish in the grooves. *Gnetaceaepollenites clathratus* Stover (form *β*) has two long, horseshoe-shaped plicae; however, the plicae pattern and the size are different.

Gnetaceaepollenites *sp. 1*
(Figures 5B, 6B)

Description. — Polyplicate, large sized grain (50–60 μm in long equatorial diameter); oblate, 10–14 inclined and partly fused plicae, and the plicae arranged in two sets on the opposite sides of grain forming the pattern A (Figure 8A). *P*/*E* ratio range from 0.5 to 0.6. Monad, symmetry bilateral, isopolar, oblate; plicae on one side are oblique to those on the other side, forming a 'checkered' pattern. Five long, horseshoe-shaped, *c.* 3–4 μm wide plicae are divided into two sets (R1, R2) of two or three long plicae. The plicae start near one tip and cross over the other tip to the opposite side of the grain, ending nearly opposite their point of origin; both ends of the two set of plicae are fused.

Dimensions. — Polar axis 28 μm, long equatorial diameter 53 μm, *P*/*E* ratio 0.52.

Occurrence. — East Xining section, Xining Basin (Late Cretaceous).

Remarks. — The plicae pattern of *Gnetaceaepollenites* sp. 1 is similar to that of *G. barghoornii*. Both have long horseshoe-shaped plicae and a 'checkered' pattern, *Gnetaceaepollenites* sp. 1 differs from *G. barghoornii* in being larger, generally almost spherical, and in having much flatter plicae as seen in transverse section.

Gnetaceaepollenites *sp. 2*
(Figures 5C, 6C, 7K)

Description. — Polyplicate, medium-large sized grain (45–60 μm in long equatorial diameter); peroblate, 10–14 spiral plicae arranged in two sets on the opposite sides of the grain forming a B-pattern (Figure 8B). *P*/E ratio range from 0.2–0.35. Monad, symmetry bilateral, isopolar, peroblate; plicae on one side are oblique to those on the other side, forming a 'checkered' pattern. The plicae arranged in two sets R1, R2, and each set of plicae start near one tip and cross over the other tip to the opposite side of the grain, ending nearly opposite their point of origin; the ends of the two set of plicae are partly fused. The plicae set R1 and R2 shared one longitudinal plica (marked with shadow parts).

Dimensions. — Polar axis 12 μm, long equatorial diameter 47 μm; *P*/*E* ratio 0.25.

Occurrence. — East Xining section, Xining Basin (Late Cretaceous).

Remarks. — This species is characterised by the elongate shape and the number of circumferential plicae that vary between two and four. There are a few short plicae that are parallel to the long plicae vanishing in the grooves near the tip.

Gnetaceaepollenites *sp. 3*
(Figures 5E, 6E, 7L)

Description. — Polyplicate, small sized grain (17 μm in long equatorial diameter); prolate, ten longitudinal flat and partly fused plicae; *P*/*E* ratio range *c*. 0.65, this species is characterised by the small size and rounded shape. Monad, symmetry bilateral, isopolar, oblate; ten longitudinal flat and partly fused plicae, *c*. 2.5 μm wide at the mid-length and gradually narrowing towards the tips; grooves *c*. 0.3 μm wide.

Dimensions. — Polar axis 11 μm, long equatorial diameter 17 μm; *P*/*E* ratio 0.64.

Occurrence. — East Xining section, Xining Basin (Late Cretaceous).

Remarks. — This species is characterised by the small size and partly fused flat plicae. *Gnetaceaepollenites uesuguii* De Lima is similar to this species, but is larger in size and has continuous circumferential plicae. The most similar to this species are the grains that Yu et al. (1983) illustrated and referred to *Ephedripites (Ephedripites) mingshuiensis* Yu, Guo et Mao. They share small size, an oval outline, and ten partly fused plicae. *Ephedripites (E.) mingshuiensis* differs from *Gnetaceaepollenites* sp. 3 in having sinuous plicae in the middle section, however this could be an artificial characteristic during the sample treatment.

Genus Steevesipollenites *Stover*

Diagnosis. — Polyplicate, ellipsoidal to fusiform pollen with a few to numerous longitudinal plicae, the exine is unusually thick at both ends compared to other ephedroids, forming expansion in the tips.

Steevesipollenites *cf.* Steevesipollenites binodosus *Stover*
(Figure 4M)

Description. — Polyplicate, large sized grain (50–60 μm in long equatorial diameter), peroblate, fusiform pollen with 10–12 plicae fused at the tips, the exine is unusually thick at both ends compared to other ephedroids, forming distinct knob, *P*/*E* ratio range from 0.3 to 0.43. Monad, symmetry bilateral, isopolar, perprolate; ten slightly sinuous plicae fused at the tips. Plicae *c*. 2 μm wide, grooves *c*. 8 μm wide; each tip has a prominent, semi-circle knob of *c*. 6 μm wide by *c*. 3 μm high.

Dimensions. — Polar axis 24 μm, long equatorial diameter 58 μm; *P*/*E* ratio 0.41.

Occurrence. — East Xining, Tiefo, and Shuiwan sections, Xining Basin (Late Cretaceous–middle to late Eocene).

Remarks. — This species is very similar to *Steevesipollenites binodosus*. These two species have the same size, but *S. binodosus* tends to have fewer but wider plicae (6–10 plicae, *c*. 2.5–4 μm). The knobs at the tips differ from each other; *S. binodosus* has prominent subspherical knobs, whereas *Steevesipollenites* cf. *S. binodosus* only has prominent semi-circle knobs.

Steevesipollenites communis *Zhang et Zhang*
(Figures 5D, 6D, 7I)

1991 *Steevesipollenites communis*, Zhang and Zhang, p1. 76, pl. 56, figs 21–24.
1999 *Steevesipollenites communis*, Song, p. 263, pl. 76, figs 14–16.

Diagnosis. — Polyplicate, medium sized grain (35–52 μm in long equatorial diameter), oblate, fusiform pollen with 10–16 fused plicae, the exine is unusually thick at both ends compared to other ephedroids, forming a distinct knob, *P*/*E* ratio range from 0.4 to 0.47.

Description. — Monad, symmetry bilateral, isopolar, oblate; fusiform pollen with 14 plicae fused at the tips that are slightly oblique to the polar axis. Plicae width is *c.* 2.5 μm at mid-length and gradually narrowing towards the tips. The exine is unusually thick at both ends, in comparison to other ephedroids, and forms a distinct knob which is *c.* 6 μm wide and *c.* 2.5 μm high.

Dimensions. — Polar axis 17 μm, long equatorial diameter 39 μm; *P*/*E* ratio 0.43.

Occurrence. — East Xining, Tiefo, and Shuiwan sections, Xining Basin (Late Cretaceous–middle to late Eocene).

Steevesipollenites cupuliformis *Azéma et Boltenhagen* (Figures 4A, 5F, 6F)

1974 *Steevesipollenites cupuliformis*, Azéma and Boltenhagen, p. 27, pl. 3, figs 1–3.
1980 *Steevesipollenites cupuliformis*, Lima, p. 41, pl. 4, figs 11–13.
1991 *Steevesipollenites cupuliformis*, Zhang and Zhang, p. 177, pl. 57, figs 15–19.
1999 *Steevesipollenites cupuliformis*, Song, p. 263, pl. 76, figs 11–13.

Diagnosis. — Polyplicate, large sized grain (40–70 μm in long equatorial diameter), peroblate, elongate shape, 8–10 straight or slightly sinuous plicae fused at the tips, the exine is unusually thick at both ends compared to other ephedroids, forming a distinct knob, *P*/*E* ratio range from 0.18 to 0.3.

Description. — Monad, symmetry bilateral, isopolar, peroblate, elongate shape, eight slightly sinuous plicae fused at the tips. Plicae are *c.* 1.5 μm wide and 4.5 μm high; the knob is *c.* 7.5 μm wide and *c.* 2 μm high.

Dimensions. — Polar axis 16 μm, long equatorial diameter 65 μm; *P*/*E* ratio 0.24.

Occurrence. — Tiefo section, Xining Basin (middle to late Eocene).

Remarks. — Both *Ephedripites (Ephedripites) montanaensis* and *Steevesipollenites cupuliformis* have the same size and the same numbers of plicae, but the plicae of *E. (E.) montanaensis* are more slender, whereas the plicae of *S. cupuliformis* have relatively rounded top as seen in transverse section. The grooves of *E. (E.) montanaensis* extend to the tips, while those of *S. cupuliformis* stop at least 2 μm from the tip. The *P*/*E* ratio of *S. cupuliformis* is smaller than that of *E. (E.) montanaensis*.

Steevesipollenites globosus *Sun et He* (Figure 4K, L)

1980 *Steevesipollenites globosus*, Sun and He, p. 99, pl. 19, figs 17–20, 28.
1987 *Steevesipollenites globosus*, Lei et al. p. 288, pl. 37, fig. 21, pl. 46, figs 23, 24.
1991 *Steevesipollenites globosus*, Zhang and Zhang, p. 177, pl. 56, figs 8–11.
1999 *Steevesipollenites globosus*, Song, p. 264, pl. 75, figs 21, 22.

Diagnosis. — Polyplicate, medium sized grain (30–40 μm in long equatorial diameter), oblate, 10–12 plicae fused at the tips, the exine is unusually thick at both ends compared to other ephedroids, forming a distinct knob, *P*/*E* ratio range from 0.6 to 0.8.

Description. — Monad, symmetry bilateral, isopolar, subspheroidal-perprolate, oval-spherical outline, ten relatively wide, straight, smooth plicae slightly oblique to the polar axis and fused at the tips. Plicae *c.* 5 μm wide at mid-length and gradually narrowing towards the tips, grooves *c.* 0.5 μm; the tip knob is *c.* 9 μm wide and *c.* 2 μm high.

Dimensions. — Polar axis 28 μm, long equatorial diameter 37 μm; *P*/*E* ratio 0.75.

Occurrence. — Tiefo, and Shuiwan sections, Xining Basin (middle to late Eocene).

Remarks. — This species is characterised by the oval-spherical outline and the relatively wide, straight plicae.

Steevesipollenites jiangxiensis *Sun et He* (Figure 4J)

1980 *Steevesipollenites jiangxiensis*, Sun and He, p. 99, pl. 19, figs 21–22, 26–27.
1991 *Steevesipollenites jiangxiensis*, Zhang and Zhang, p. 178, pl. 57, figs 1–3, 5.
1999 *Steevesipollenites jiangxiensis*, Song, p. 265, pl. 75, figs 15–16.

Diagnosis. — Polyplicate, medium sized grain (30–40 μm in long equatorial diameter), oblate, 7–11 plicae fused at the tips, the exine is unusually thick at both ends compared to other ephedroids, forming a distinct knob, *P*/*E* ratio range from 0.5 to 0.7.

Description. — Monad, symmetry bilateral, isopolar, oblate, fusiform pollen with ten straight, wide plicae that are fused at the tips. Plicae *c.* 5 μm wide at mid-length and gradually narrowing towards the tips, three relatively slender plicae (2.5 μm wide) are strongly waved, grooves *c.* 0.5 μm wide, the knob is *c.* 6.5 μm wide and *c.* 1.5 μm high.

Dimensions. — Polar axis 23 μm, long equatorial diameter 40 μm; *P*/*E* ratio 0.57.

Occurrence. — Tiefo and Shuiwan section, Xining Basin (middle to late Eocene).

Remarks. — This species is similar to *Steevesipollenites globosus*, but *S. jiangxiensis* has relatively smaller *P*/*E* ratio and sinuous plicae. The sinuous plicae might be an artificial character due to the treatment; however, given that not all the plicae of the grain are strongly sinuous, they may represent a true diagnostic characteristic of this species.

Steevesipollenites major *Zhang et Zhang* (Figure 4I)

1991 *Steevesipollenites major*, Zhang and Zhang, p. 178, pl. 56, fig. 33.
1999 *Steevesipollenites major*, Song, p. 265, pl. 77, fig. 27.

Diagnosis. — Polyplicate, large sized grain (70–75 μm in long equatorial diameter), peroblate, 10–14 plicae fused at the tips, the exine is unusually thick at both ends compared to other ephedroids, forming a distinct knob, *P*/*E* ratio range from 0.3 to 0.5.

Description. — Monad, symmetry bilateral, isopolar, peroblate, fusiform pollen with 12 spiral and wide plicae, fused at the tips. Plicae on one side oblique to those on the other side forming a 'checkered' pattern; plicae *c.* 5.5 μm wide at mid-length and gradually narrowing towards the tips, the knob is *c.* 9.5 μm wide and *c.* 1.5 μm high.

Dimensions. — Polar axis 35 μm, long equatorial diameter 73 μm; *P*/*E* ratio 0.48.

Occurrence. — Tiefo and Shuiwan section, Xining Basin (middle to late Eocene).

Remarks. — This species differs from other species in having a larger size (> 70 μm in long equatorial diameter).

Changes in Gnetales composition through time

Our palynological records show that the morphological changes of ephedroid pollen in northern Tibet can be divided at least into four stages (Figure 9; Herb et al. 2013). During the late Early Cretaceous, ephedroid pollen is predominantly represented by *Gnetaceaepollenites* (more than 85%), with low percentages of *Ephedripites* subgen. *Ephedripites* (*c.* 10%) and *Steevesipollenites* (less than 2%), and rare *Ephedripites* subgen. *Distachyapites*. In the late Late Cretaceous–early Palaeogene, the ephedroid pollen assemblage is dominated by increased percentages of *Ephedripites* subgen. *Ephedripites* (*c.* 20%), higher percentages of *Ephedripites* subgen. *Distachyapites* (*c.* 15%) than in the late Early Cretaceous, and slightly higher percentages of *Steevesipollenites* (*c.* 3%); notably *Gnetaceaepollenites* is no longer present. During the middle to late Eocene, *Ephedripites* comprises about 20–60% of the total pollen composition, with a predominance of *Ephedripites* subgen. *Distachyapites*.

We subdivided the middle to late Eocene palynological record into two *Ephedripites* zones (Fig-Figure 10). Zone I is composed of *Ephedripites* subgen. *Distachyapites* (60–80%), *Ephedripites* subgen. *Ephedripites* (5–20%) and *Steevesipollenites* (5–15%). Within this zone, some species with highly diverse branched pseudosulci and a larger *P*/*E* ratio (such as *Ephedripites [Distachyapites] fushunensis, E. [D.] claricristatus* and *E. [D.] lusaticus*) occur in relatively high percentages (5–25%). Zone II is dominated by *Ephedripites* subgen. *Distachyapites* (more than 90%) and the percentage of species with less branched pseudosulci (i.e. *E. [D.] fusiformis, E. [D.] longiformis*) increase, whereas the percentages of *Ephedripites* subgen. *Ephedripites* (less than 10%) and *Steevesipollenites* (less than 5%) decrease sharply.

Finally, in the Qaidam Basin, *Ephedripites* percentages of around 10% or less of the total pollen composition (Herb et al. 2013) are recorded in the Quaternary deposits. These values are in stark contrast with the Eocene interval. In the Quaternary deposits, only two types of *Ephedra* pollen were found and both are equivalent to the derived type as described by Bolinder et al. (2016), but with poorly developed first-order branches of the pseudosulci. As yet no quantitative data are available for the latest Paleogene and Neogene deposits in our sections.

Changes in Cenozoic steppe composition through time

The Late Cretaceous–early Palaeogene pollen assemblages are characterised by ~40% presence of typical steppe taxa (Figure 9), which are mainly

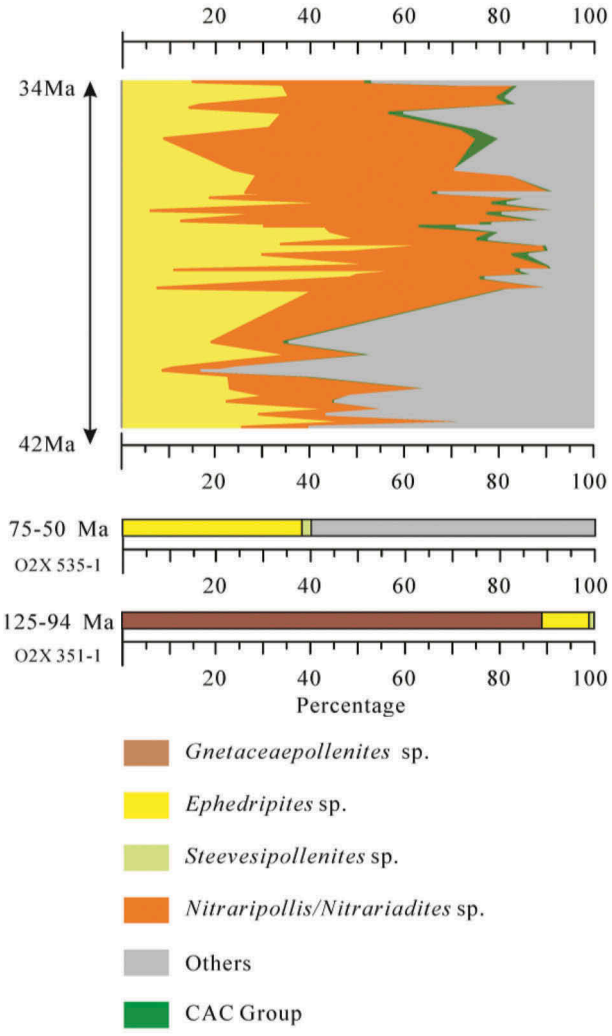

Figure 9. Cumulative diagrams showing pollen of steppe type vegetation versus that of other taxa from the Late Cretaceous to the Eocene in the Xining Basin. Little *Ephedripites* subgen. *Distachyapites* occurred during the late Early Cretaceous, whereas *Gnetaceaepollenites* did not. The percentage of *Ephedripites* subgen. *Distachyapites* has increased since the late Late Cretaceous–early Palaeogene, and the amount of *Steevesipollenites* decrease after that time. *Ephedripites* subgen. *Distachyapites* and *Nitraripollis/Nitrariadites* sp. increased considerably and dominated the steppe vegetation of the late Eocene.

composed of *Ephedripites*. In the middle Eocene (here *c.* 42–40 Ma; Lutetian–Bartonian, comprising 47.8–37.8 Ma), the steppe taxa are made up of *Ephedripites* (25–40%) and *Nitraripollis/Nitrariadites* (10–30%), which account for ~50% of the pollen sum. In contrast, in the middle to late Eocene (here *c.* 40–34 Ma; Priabonian, comprising 37.8–33.9 Ma), steppe pollen dominates the pollen sum (~80%). The base of this time interval is rich in *Ephedripites* pollen (up to 60%), whereas *Nitraripollis/Nitrariadites* becomes dominant at the top (25–60%). Also the pollen of Chenopodiaceae, Amaranthaceae and Caryophyllaceae (CAC group) appear during this period, although their percentages do not exceed ~5% of the pollen sum. During the Quaternary in the Qaidam Basin, steppe taxa account for ~80% of the pollen sum, but, contrary to the Eocene situation, pollen of the CAC group dominates the pollen assemblage (around 60%) and percentages of *Ephedripites* pollen are low (~12%) and *Nitraripollis/Nitrariadites* is rare.

Discussion

Morphology and abundance of ephedroid pollen in the Cretaceous–Eocene strata of the Xining Basin

Generally, both *Ephedripites* and *Equisetopollenites* are used to describe pollen grains with affinity to *Ephedra*. Considering the possibility of confusion and the unsuitability of the name *Equisetopollenites*, we choose to use *Ephedripites* to describe pollen with tip-fused plicae. Based on the presence or absence of side branches on the pseudosulci, *Ephedripites* can be grossly divided into two groups: pollen grains with branched pseudosulci classified in *Ephedripites* subgen. *Distachyapites*, and pollen grains with unbranched pseudosulci, which traditionally have been subdivided into *Ephedripites* subgen. *Ephedripites* (straight plicae) and *Ephedripites* subgen. *Spiralipites* (spiral plicae). Recent work on modern pollen indicates, however, that the spiral form is frequently found intermingled with straight forms in the same microsporangium (Norbäck-Ivarsson 2014) and the division of pollen with unbranched pseudosulci into the two subgenera *Ephedripites* subgen. *Ephedripites* and *Ephedripites* subgen. *Spiralipites* is most probably artificial and redundant. Furthermore, only a few pollen grains of the spiral form have been found in the Late Cretaceous strata of the Xining Basin. From the Cretaceous to the Eocene, *Ephedripites* subgen. *Ephedripites* and *Ephedripites* subgen. *Distachyapites* occur during every epoch, but the percentage of *Ephedripites* subgen. *Ephedripites* is higher in the Late Cretaceous–Paleocene than in the Eocene. By contrast, the diversity and abundance of *Ephedripites* subgen. *Distachyapites* expands rapidly during the Paleocene, reaching its maximum in the Eocene, and decline after the Eocene–Oligocene boundary. In the samples from the Quaternary and the present, the percentages of ephedroids are even lower. Although this suggests a further decline of ephedroid pollen in the Xining Basin from the early Oligocene onwards, it should be noted that there are currently no available data from the Neogene in this basin. *Steevesipollenites*, which has fused plicae and an exine that is unusually thick at both ends (if compared to other ephedroids), was found in the Late

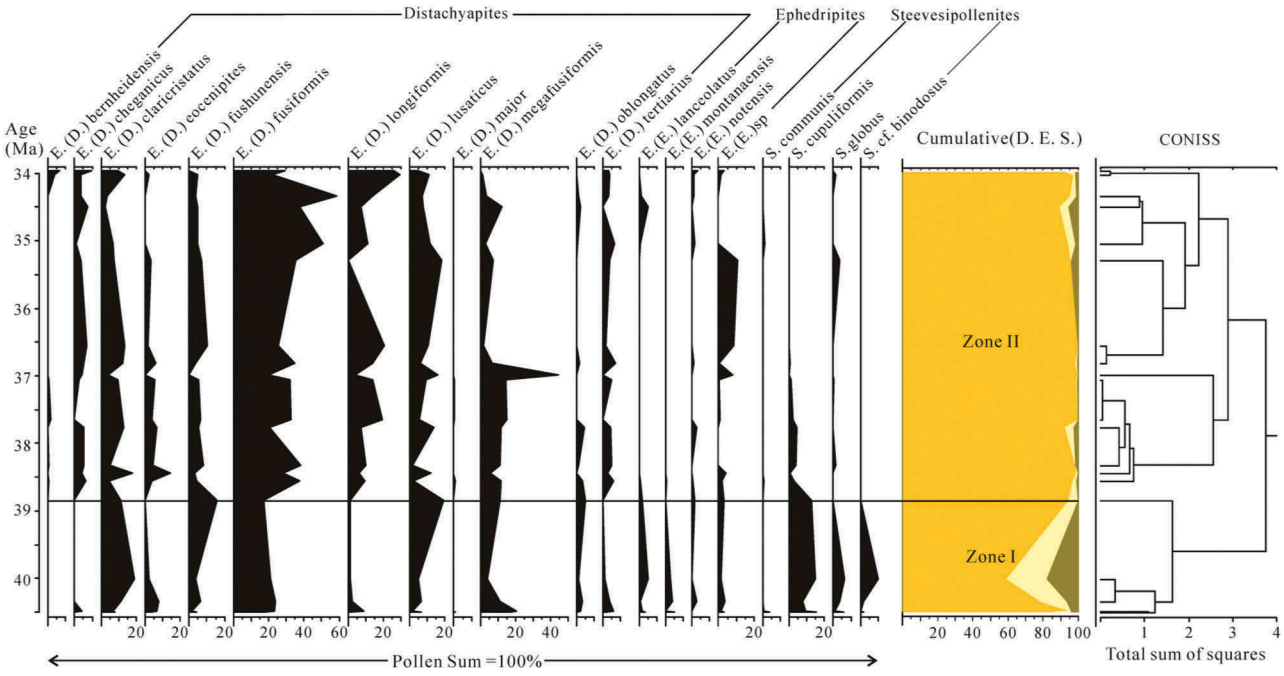

Figure 10. Eocene ephedroid pollen composition diagram in the Xining Basin. Zone I is characterised by a mix of *Ephedripites* subgen. *Ephedripites* and *Ephedripites* subgen. *Distachyapites* and *Steevesipollenites*. *Ephedripites* subgen. *Distachyapites* dominates Zone II while *Ephedripites* subgen. *Ephedripites* decreased. The changes in ephedroid pollen composition (Zones I–II) coincide with aridification phases observed in Hoorn et al. (2012) and Bosboom et al. (2014a).

Cretaceous–Eocene strata. It occurs in relatively high percentages in the Late Cretaceous–Paleocene and declines in the Eocene.

On the confusion of Gnetaceaepollenites *and* Schizaeoisporites

As for the pollen with none-fused or partly fused plicae, we choose to call them *Gnetaceaepollenites* following De Lima (1979a). According to the original description (Jansonius & Hills 1980), *Schizaeoisporites* are monolete spores with plicae converged at the two narrow ends, and the monolete mark enclosed by plicae. Similar grains are called *Schizaeoisporites* in the Cretaceous strata of China (Song 1978, 1999; Zhu et al. 1985; Wang et al. 1990; Zhang & Zhan 1991) because the plicae are not fused at the narrow ends and the laesura is difficult to see. In this study, 24 grains of this pollen type (previously assigned to *Schizaeoisporites*, see earlier) were examined by means of SEM. In none of these grains, a laesura was found; we consequently suggest that they are pollen, not spores, and belong to *Gnetaceaepollenites*.

Ephedroid pollen types and paleoenviromental change

In the Xining study area, both lithofacies and pollen assemblages indicate rapid aridification during the middle Eocene (~40 Ma; Bosboom et al. 2014a). This aridification might be associated with a change in monsoonal intensity related to regional tectonic uplift as well as global climate and land-sea distribution changes (Quan et al. 2011; Licht et al. 2014; Bosboom et al. 2014b). The aridification is not only recorded in the Xining Basin, but also in the neighbouring Qaidam Basin (Rieser et al. 2009; Song et al. 2013) and it coincides with changes in ephedroid pollen composition (Zones I–II; Figure 10) as documented in our study.

It has been previously reported that *Ephedra* grains shrink by polar contraction under dry conditions; the grooves become deeper and narrower and the plicae become less arched and closer together (Wodehouse 1935), which yields a smaller *P*/*E* ratio. By contrast, under moist conditions, the grains expand and the plicae flatten out (Wodehouse 1935) and the *P*/*E* ratio is larger. We suggest that the development of branched pseudosulci as shown in *Ephedripites* subgen. *Distachyapites* could have evolved as an adaptation to a dryer climate and perhaps also to a different pollination syndrome as suggested by Bolinder et al. (2015). Zone I is characterised by a mix of *Ephedripites* subgen. *Ephedripites* and *Ephedripites* subgen. *Distachyapites*. The crenate margin of some species (*E. [D.] fushunensis, E. [D.] claricristatus, E. [D.] cheganica*) may be caused by the flattening of plicae and protruding grooves, which in addition to the relatively high percentages of species with a large *P*/*E* ratio indicates a relatively humid

climate. In zone II, *Ephedripites* subgen. *Distachyapites* dominates while *Ephedripites* subgen. *Ephedripites* has decreased. The percentage of species with smaller *P*/*E* ratio, especially *E. (D.) longiformis* (Figure 10), is abundant within this zone, which indicates a dryer environment.

Notably, the presence of *Ephedripites* subgen. *Distachyapites* (*E. eocenipites, E. fusiformis, E. lusaticus* and *E. claricristatus*) has also been observed in the Cenozoic record in the sedimentary basins of southern Brazil, albeit in much lower percentages than in the Tibetan sections (Garcia et al. 2016). Nevertheless this points at a global distribution of these taxa, a matter that deserves further study.

Conclusions

Our data indicate that the steppe vegetation in the Tibetan Plateau changed significantly from the Late Cretaceous to the Oligocene. The ephedroid pollen record in the Xining Basin suggests that the genus *Gnetaceaepollenites*, which is abundant in the Cretaceous, went extinct in association with the Cretaceous–Paleogene (K–Pg) boundary. *Ephedripites* subgen. *Ephedripites* and *Steevesipollenites* are also common in the Cretaceous. Both *Ephedripites* subgen. *Ephedripites* and *Ephedripites* subgen. *Distachyapites* were highly diverse in the Paleocene–middle Eocene, together with small percentages of *Steevesipollenites*. Around 40 Ma, *Ephedripites* subgen. *Distachyapites* increased considerably and dominated the steppe vegetation at least until the late Eocene, while *Ephedripites* subgen. *Ephedripites* and *Steevesipollenites* decreased. In contrast, during the Quaternary, the steppe vegetation in the Qaidam Basin is mainly composed of *Artemisia* and Chenopodiaceae accompanied by Poaceae, Cyperaceae and Asteraceae and relatively low percentages and a low diversity of Ephedraceae. We hypothesise that these temporal changes in composition of ephedroid pollen are linked to regional as well as global climatic changes. The regional aridification in the Xining Basin during the middle to late Eocene might have played an important role in the diversification of *Ephedripites* subgen. *Distachyapites* and the posterior drop in diversity and relative abundance of *Ephedripites* may be linked to the global cooling leading to the Eocene–Oligocene transition.

Acknowledgements

The authors thank Jan van Arkel, Institute for Biodiversity and Ecosystem Dynamics, University of Amsterdam, Amsterdam, The Netherlands, for microphotography, Annemarie Philip, Institute for Biodiversity and Ecosystem Dynamics, University of Amsterdam, Amsterdam, The Netherlands, for palynological processing and Brian Horton, Department of Earth and Space Sciences, University of California, Los Angeles, California, USA, for sharing samples and palynological slides. The study on the evolution of *Ephedra* is a partnership between the universities of Amsterdam (The Netherlands), Stockholm (Sweden) and Wuhan (China).

Disclosure statement

No potential conflict of interest was reported by the authors.

Funding

Funding was provided from the Swedish Research Council VR to CR and the Geological Survey of China [No.1212011121261] to K. Zhang. The study of the SG-1 core sediments was funded by the German Research Foundation (PR651/8) to Jörg Pross.

ORCID

Catarina Rydin http://orcid.org/0000-0002-3347-7820

References

Abels HA, Dupont-Nivet G, Xiao G, Bosboom R, Krijgsman W. 2011. Step-wise change of Asian interior climate preceding the Eocene–Oligocene Transition (EOT). Palaeogeography, Palaeoclimatology, Palaeoecology 299: 399–412. doi:10.1016/j.palaeo.2010.11.028.

Abubakar MB, Luterbacher HP, Ashraf AR, Ziedner R, Maigari AS. 2011. Late Cretaceous palynostratigraphy in the Gongola Basin (Upper Benue Trough, Nigeria). Journal of African Earth Sciences 60: 19–27. doi:10.1016/j.jafrearsci.2011.01.007.

Akkiraz MS, Kayseri MS, Akgün F. 2008. Palaeoecology of coal-bearing Eocene sediments in Central Anatolia (Turkey) based on quantitative palynological data. Turkish Journal of Earth Sciences 17: 317–360.

Anderson RY. 1959. Cretaceous-Tertiary palynology of the eastern side of the San Juan Basin, 147. New Mexico: School of Mineral Sciences.

Azéma C, Boltenhagen E. 1974. Pollen du Crétacé moyen du Gabon attribué aux Ephedrales. Lille: Laboratoire de paléobotanique, Université des sciences et techniques, Villeneuve d'Ascq.

Baltes N. 1966. Palynological note on Cretaceous deposits of the Tano Basin (Ghana). Proceedings of the 2nd West African Micropaleontological Colloquium, Ibadan, Nigeria, 18 June–1 July 1965, 3–6.

Belsky CY, Jardiné S, Prestat B, Durif P, Grosdidier E, Cassan JP, Gillmann M. 1975. Etude stratigraphique et sédimentologique d'une coupe du Crétacé-Tertiaire au large du Suriname. Proceedings of the Ninth Inter-Guyana Geological Conference. Ciudad Guayana, Venezuela, 7–14 May 1972, 179–187.

Bercovici A, Hadley A, Villanueva-Amadoz U. 2009. Improving depth of field resolution for palynological photomicrography. Palaeontologia Electronica 12: 1–12.

Bharadwaj D. 1963. Pollen grains of *Ephedra* and *Welwitschia* and their probable fossil relatives. Memoirs of the Indian Botanical Society 4: 125–135.

Bolinder K, Ivarsson LN, Humphreys AM, Ickert-Bond SM, Han F, Hoorn C, Rydin C. 2016. Pollen morphology of *Ephedra* (Gnetales) and its evolutionary implications. Grana 1–28. doi:10.1080/00173134.2015.1066424.

Bolinder K, Niklas KJ, Rydin C. 2015. Aerodynamics and pollen ultrastructure in *Ephedra* (Gnetales). American Journal of Botany 102: 457–470. doi:10.3732/ajb.1400517.

Bolkhovitina N. 1953. Characteristic spores and pollen grains of Cretaceous of Central region of USSR. Transactions of the Institute of Geology, Akademia Nauk SSSR 61: 1–184.

Bolkhovitina N. 1961. Spores fossiles et actuelles de la famille des Schizeaceae. Transactions of the Institute of Geology, Akademia Nauk SSSR 40: 1–165.

Bosboom RE, Abels HA, Hoorn C, Bcj VDB, Guo Z, Dupont-Nivet G. 2014a. Aridification in continental Asia after the Middle Eocene Climatic Optimum (MECO). Earth and Planetary Science Letters 389: 34–42. doi:10.1016/j.epsl.2013.12.014.

Bosboom RE, Dupont-Nivet G, Grothe A, Brinkhuis H, Villa G, Mandic O, Stoica M, Huang W, Yang W, Guo Z, Krijgsman W. 2014b. Linking Tarim Basin sea retreat (west China) and Asian aridification in the late Eocene. Basin Research 26: 621–640. doi:10.1111/bre.12054.

Brenner GJ. 1968. Middle Cretaceous spores and pollen from northeastern Peru. Pollen et Spores 10: 341–383.

Brenner GJ. 1976. Middle Cretaceous floral provinces and early migration of angiosperms. In: Beck CB, ed. Origin and early evolution of angiosperms. New York: Columbia University Press.

Brown CW, Pierce RL. 1962. Palynologic correlations in Cretaceous Eagle Ford Group, northeast Texas. American Association of Petroleum Geologists Bulletin 46 (12): 2133–2147.

Caveney S, Charlet DA, Freitag H, Maier-Stolte M, Starratt AN. 2001. New observations on the secondary chemistry of world *Ephedra* (Ephedraceae). American Journal of Botany 88: 1199–1208. doi:10.2307/3558330.

Chlonova AF. 1961. Spores and pollen of upper part of the Upper Cretaceous of the eastern part of the western Siberian lowland. Transactions Institute Geology Akademi Nauka SSSR 7: 1–138.

Chlonova AF, Strepetilova VG, Purrova SI, Strepetilova TG. 1994. Changes in composition of palynological assemblages from Cretaceous deposits of the eastern part of the West Siberian Plain. Cretaceous Research 15: 435–444. doi:10.1006/cres.1994.1025.

Cookson IC. 1956. Pollen grains of the *Ephedra* type in Australian Tertiary deposits. Nature 177: 47–48. doi:10.1038/177047a0.

Crane PR, Maisey JG. 1991. Fossil plants. In Maisey JG, ed. Santana fossils: An illustrated atlas, 414–419. Neptune, NJ: TFH Publications Inc.

Dai S, Fang X, Dupont-Nivet G, Song C, Gao J, Krijgsman W, Langereis C, Zhang W. 2006. Magnetostratigraphy of Cenozoic sediments from the Xining Basin: Tectonic implications for the northeastern Tibetan Plateau. Journal of Geophysical Research: Solid Earth 111: 1–19. doi:10.1029/2005JB004187.

Daugherty LH. 1941. The Upper Triassic flora of Arizona. Washington: Carnegie Institution of Washington Publication.

Davis ME. 2005. Forcing of the Asian monsoon on the Tibetan Plateau: Evidence from high-resolution ice core and tropical coral records. Journal of Geophysical Research 110: 1–13. doi:10.1029/2004JD004933.

De Lima MR 1978a. Palinologia da Formacão Santana (Cretáceo do nordeste do Brasil). PhD dissertation, Universidade de São Paulo, São Paulo, Brazil.

De Lima MR. 1978b. Microfósseis da Formação Exu, Cretáceo do nordeste do Brasil. Anais do 30° Congresso Brasileiro de Geologia Recife 2: 965–969.

De Lima MR. 1979a. Palinologia da Formacão Santana (Cretáceo do nordeste do Brasil). III. Descricão sistemática dos esporos da subturma *Zonotriletes* e turma *Monoletes*, e dos polenas das Turmas Saccites e Aletes. Ameghiniana 16: 27–63.

De Lima MR. 1979b. Paleontologia da Formação Santana (Cretáceo do nordeste do Brasil): Estágio atual de conhecimentos. Anais da Academia Brasileira de Ciências 51: 545–556.

De Lima MR. 1980. Palinologia da Formação Santana (Cretáceo do nordeste do Brasil). III. Descrição sistemática dos polens da Turma Plicates (Subturma Costates). Ameghiniana 17: 15–47.

De Lima MR. 1981. Palinologia do Mesozóico brasileiro: Uma síntese. In: Volkheimer W, ed. Cuencas sedimentarias del Jurásico y Cretácico de América del Sur, Vol. 2, 445–460. Buenos Aires, Argentina: Universidad de Buenos Aires.

De Lima MR. 1982. Palinologia da Formação Codó na Região de Codó, Maranhão. Boletim, Instituto de Geociéncias, Universidade de São Paulo, Série Cientifica 13: 116–128.

De Lima MR. 1984. Palinologia do linhito de Jatoba (Cretáceo do nordeste do Brasil). I. Introdução, contexto estratigrafico, identificação de species cretáceas. Anais 33° Congresso Brasileiro de Geologia, Rio de Janeiro, October 1984, 2: 536–547.

De Lima MR, Coelho MPCA. 1987. Estudo palinologico da sondagem estratigráfica de Lagoa do Forno, Bacia do Rio do Peixe, Cretáceo do nordeste do Brasil. Boletim, Instituto de Geociências, Universidade de São Paulo, Série Cientifica 18: 67–83.

De Lima MR, Perinotto JA. 1984. Palinologia de sedimentos da parte superior da Formação Missão Velha, Bacia do Araripe. Geociências (São Paulo) 3: 67–76.

Dilcher DL, Bernardes-De-Oliveira ME, Pons D, Lott TA. 2005. Welwitschiaceae from the lower Cretaceous of northeastern Brazil. American Journal of Botany 92: 1294–1310. doi:10.3732/ajb.92.8.1294.

Dino R. 1992. Palinologia, bioestratigrafia e paleoecologia da Formação Alagamar, Cretáceo da Bacia Potiguar, nordeste do Brasil. PhD dissertation, Universidade de São Paulo, Brazil.

Dino R. 1994. Algunas espécies novas de grãos de pollen do Cretáceo inferior do nordeste do Brasil. Boletim de Geociéncias da Petrobrás 8: 79–98.

Dino R, Pocknall DT, Dettmann ME. 1999. Morphology and ultrastructure of elater-bearing pollen from the Albian to Cenomanian of Brazil and Ecuador: Implications for botanical affinity. Review of Palaeobotany and Palynology 105: 201–235. doi:10.1016/S0034-6667(98)00076-1.

Duan Q, Zhang K, Wang J, Yao H, Pu J. 2007. Sporopollen assemblage from the Totohe Formation and its stratigraphic significance in the Tanggula Mountains, northern Tibet. Earth Science Journal of China University of Geosciences 32: 623–637.

Dupont-Nivet G, Hoorn C, Konert M. 2008. Tibetan uplift prior to the Eocene–Oligocene climate transition: Evidence from pollen analysis of the Xining Basin. Geology 36: 987–990. doi:10.1130/G25063A.1.

Dupont-Nivet G, Krijgsman W, Langereis CG, Abels HA, Dai S, Fang X. 2007. Tibetan plateau aridification linked to global cooling at the Eocene–Oligocene transition. Nature 445: 635–638. doi:10.1038/nature05516.

EB L, Pakiser HM. 1964. A preliminary report on the pollen and spores of the pre-Selma Upper Cretaceous strata of western Alabama. Geological Survey Bulletin 1160: 71–95.

El-Ghazaly G, Rowley JR. 1997. Pollen wall of *Ephedra foliata*. Palynology 21: 7–18. doi:10.1080/01916122.1997.9989483.

Frederiksen NO. 1973. New mid-Tertiary spores and pollen grains from Mississippi and Alabama. Tulane Studies in Geology and Paleontology 10: 65–86.

Fu L, Yu Y, Harald R. 1999. Flora of China. Beijing: Science Press.

Garcia MJ, Premaor E, Deoliveira PE, Bernardes-de-Oliveira MEC, Rodolfo D, Antonioli L, De Menezes JB. 2016. Cenozoic

distribution of *Ephedripites* Bolkhovitina (1953) ex Potonié (1958) emend. Krutzsch (1961) in Brazil. Grana 55: 52–70. doi:10.1080/00173134.2015.1119882.

Ghosh AK, Banerji D, Srivastava SK. 1963. *Ephedra*-type pollen grains in the Dharamsala (Tertiary) Formations, Punjab, India. Nature 198: 408. doi:10.1038/198408a0.

Graham A. 1965. The Sucker Creek and Trout Creek Miocene floras of southeastern Oregon. Ohio: Kent State University Press.

Gray J. 1960. Temperate pollen genera in the Eocene (Claiborne) flora, Alabama. Science 132: 808–810. doi:10.1126/science.132.3430.808.

Grimm EC. 1987. CONISS: A FORTRAN 77 program for stratigraphically constrained cluster analysis by the method of incremental sum of squares. Computers & Geosciences 13: 13–35. doi:10.1016/0098-3004(87)90022-7.

Guo X, Wang N, Ding X, Zhao M, Wang D. 2006. Discovery of Paleogene palynological assemblages from the Wanbaogou Group-complex in western part of the eastern Kunlun orogenic belt and its geological significance. Science in China Series D 49 (4): 358–367.

Hedlund RW. 1966. Palynology of the Red Branch Member of the Woodbine Formation (Cenomanian), Bryan County. Oklahoma: University of Oklahoma.

Herb C, Appel E, Voigt S, Koutsodendris A, Pross J, Zhang W, Fang X-M. 2015. Orbitally tuned age model for the late Pliocene–Pleistocene lacustrine succession of drill core SG-1 from the western Qaidam (NE Tibetan Plateau). Geophysical Journal International 200: 35–51. doi:10.1093/gji/ggu372.

Herb C, Zhang W, Koutsodendris A, Appel E, Fang X-M, Pross J. 2013. Environmental implications of the magnetic record in Pleistocene lacustrine sediments of the Qaidam Basin, NE Tibetan Plateau. Quaternary International 313-314: 218–229. doi:10.1016/j.quaint.2013.06.015.

Herngreen GFW. 1973. Palynology of Albian–Cenomanian strata of borehole 1-QS-1-MA, state of Maranhão, Brazil. Pollen et Spores 15: 515–545.

Herngreen GFW. 1974. Middle Cretaceous palynomorphs from northeastern Brazil. Results of a palynological study of some boreholes and comparison with Africa and the Middle East. Sciences Géologiques Bulletin 27: 101–116.

Herngreen GFW. 1975. Palynology of Middle and Upper Cretaceous strata in Brazil. Mededelingen Rijks Geologische Dienst N.S. 26: 39–91.

Herngreen GFW. 1981. Microfloral relationships between Africa and South America in Middle and Upper Cretaceous time. IV International Palynological Conference 3: 406–417.

Herngreen GFW, Chlonova AF. 1981. Cretaceous microfloral provinces. Pollen et Spores 23: 441–555.

Herngreen GFW, Duenãs Jimenez H. 1990. Dating of the Cretaceous Une Formation, Colombia and the relationship with the Albian-Cenomanian African-South American microfloral province. Review of Palaeobotany and Palynology 66: 345–359.

Hesse M, Halbritter H, Weber M, Buchner R, Frosch-Radivo A, Ulrich S. 2009. Pollen terminology: An illustrated handbook. Vienna: Springer.

Hochuli PA. 1981. North Gondwanan floral elements in lower to middle Cretaceous sediments of the Southern Alps (southern Switzerland, northern Italy). Review of Palaeobotany and Palynology 35: 337–358. doi:10.1016/0034-6667(81)90116-0.

Hoorn C, Straathof J, Abels HA, Xu Y, Utescher T, Dupont-Nivet G. 2012. A late Eocene palynological record of climate change and Tibetan Plateau uplift (Xining Basin, China). Palaeogeography, Palaeoclimatology, Palaeoecology 344-345: 16–38. doi:10.1016/j.palaeo.2012.05.011.

Horton BK, Dupont-Nivet G, Zhou J, Waanders GL, Butler RF, Wang J. 2004. Mesozoic–Cenozoic evolution of the Xining-Minhe and Dangchang basins, northeastern Tibetan Plateau: Magnetostratigraphic and biostratigraphic results. Journal of Geophysical Research 109: 1–15. doi:10.1029/2003JB002913.

Huynh K-L. 1975. Le probléme de la polarité du pollen d'*Ephedra*. Pollen et Spores 16: 469–474.

Jansonius J. 1962. Palynology of Permian and Triassic sediments, Peace River area, western Canada. Palaeontographica Abt. B 110: 35–98.

Jansonius J, Hills LV. 1980. Genera file of fossil spores. Calgary: University of Calgary.

Jaramillo CA, Dilcher DL. 2001. Middle Paleogene palynology of Central Colombia. South America: A study of pollen and spores from tropical latitudes. Palaeontographica Abt. B 258: 87–213.

Jarzen DM, Dilcher DL. 2006. Middle Eocene terrestrial palynomorphs from the Dolime Minerals and Gulf Hammock quarries, Florida, USA. Palynology 30: 89–110.

Kedves M. 1987. LM and EM studies on pollen grains of recent *Welwitschia mirabilis* Hook and *Ephedra* species. Acta Botanica Hungarica 33: 81–103.

Kirchheimer F. 1950. Mikrofossilien aus Salzablageaungen des Tertiärs. Palaeontographica 90: 127–160.

Krutzsch W. 1961. Über Funde von "ephedroidem" Pollen im deutschen Tertiär. Geologie 10: 15–53.

Krutzsch W. 1970. Atlas der mittel- und jungtertiären dispersen Sporen- und Pollen- sowie der Mikroplanktonformen des nördlichen Mitteleuropas, Lieferung VII. Berlin: Deutscher Verlag der Wissenschaften.

Kurmann MH, Zavada MS. 1994. Pollen morphological diversity in extant and fossil gymnosperms. In: Kurmann MH, Doyle JA, eds. Ultrastructure of fossil spores and pollen, 123–137. London: Kew Royal Botanic Gardens.

Kutzbach J, Prell W, Ruddiman WF. 1993. Sensitivity of Eurasian climate to surface uplift of the Tibetan Plateau. The Journal of Geology 101: 177–190. doi:10.1086/jg.1993.101.issue-2.

Leier AL, DeCelles PG, Pelletier JD. 2005. Mountains, monsoons, and megafans. Geology 33: 289. doi:10.1130/G21228.1.

Li D. 2008. Floristics and plant biogeography in China. Journal of Integrative Plant Biology 50: 771–777. doi:10.1111/jipb.2008.50.issue-7.

Li M. 1989. Sporo-pollen from Shanghu Formation of early Peleocene in Nanxiong Basin, Guangdong. Acta Palaeontologica Sinica 28: 741–750.

Li J, Batten DJ, Zhang Y. 2008. Late Cretaceous palynofloras from the southern Laurasian margin in the Xigaze region, Xizang (Tibet). Cretaceous Research 29: 294–300. doi:10.1016/j.cretres.2007.05.002.

Li J, Fang X, Song C, Pan B, Ma Y, Yan M. 2014. Late Miocene–Quaternary rapid stepwise uplift of the NE Tibetan Plateau and its effects on climatic and environmental changes. Quaternary Research 81: 400–423. doi:10.1016/j.yqres.2014.01.002.

Licht A, Van Cappelle M, Abels H, Ladant JB, Trabucho-Alexanfre J, France-Lanord C, Donnadieu Y, Vandenberghe J, Rigaudier T, Lécuyer C. 2014. Asian monsoons in a late Eocene greenhouse world. Nature 513: 501–506. doi:10.1038/nature13704.

Liu X, Yin Z. 2002. Sensitivity of East Asian monsoon climate to the uplift of the Tibetan Plateau. Palaeogeography, Palaeoclimatology, Palaeoecology 183: 223–245. doi:10.1016/S0031-0182(01)00488-6.

Lu H, Guo Z. 2013. Evolution of the monsoon and dry climate in East Asia during late Cenozoic: A review. Science China Earth Sciences 57: 70–79. doi:10.1007/s11430-013-4790-3.

Ma Y, Li J, Fang X. 1998. Palynoflora and climatic evolution records from red-beds (30.6–5.0 Ma) in Lin-Xia Area. Chinese Science Bulletin 43: 301–304.

Mabesoone JM, Tinoco IM. 1973. Palaeoecology of the Aptian Santana Formation (northeastern Brazil). Palaeogeography, Palaeoclimatology, Palaeoecology 14: 97–118.

Markevich VS, Mozherovskii AV, Terekhov EP. 2012. Palynological characteristics of the sediments of the Malokuril'skaya formation (Maastrichtian-Danian), Shikotan Island. Stratigraphy and Geological Correlation 20 (5): 466–477.

Miao Y, Wu F, Chang H, Fang X, Deng T, Sun J, Jin C. 2015. A Late–Eocene palynological record from the Hoh Xil Basin, northern Tibetan Plateau, and its implications for stratigraphic age, paleoclimate and paleoelevation. Gondwana Research. doi:10.1016/j.gr.2015.01.007.

Miao YF, Fang XM, Wu FL, Cai MT, Song CH, Meng QQ, Xu L. 2013a. Late Cenozoic continuous aridification in the western Qaidam Basin: Evidence from sporopollen records. Climate of the Past 9 (4): 1863–1877.

Miao Y, Wu F, Herrmann M, Yan X, Meng Q. 2013b. Late early Oligocene East Asian summer monsoon in the NE Tibetan Plateau: Evidence from a palynological record from the Lanzhou Basin, China. Journal of Asian Earth Sciences 75: 46–57. doi:10.1016/j.jseaes.2013.07.003.

Miao Y, Yan X, Shao Y, Yang B. 2011. Cenozoic Ephedraceae adaptation to global cooling in northwestern China. Sciences in Cold and Arid Regions 3: 375–380.

Mildenhall DC, Kennedy EM, Lee DE, Kaulfuss U, Bannister JM, Fox B, Conran JG. 2014. Palynology of the early Miocene Foulden Maar, Otago, New Zealand: Diversity following destruction. Review of Palaeobotany and Palynology 204: 27–42.

Müller H. 1966. Palynological investigations of Cretaceous sediments in northeastern Brazil. Proceedings of the 2nd West African Micropaleontological Colloquium, Ibadan, Nigeria, 18 June–1 July 1965, 123–136

Muller J. 1968. Palynology of the Pedawan and plateau sandstone formations (Cretaceous–Eocene) in Sarawak, Malaysia. Micropaleontology 14: 1–37. doi:10.2307/1484763.

Nagy E. 1963. Occurrence of the genus *Ephedripites* in the Neogene of Hungary. Grana 4 (2): 277–280.

Narváez PL, Sabino IF. 2008. Palynology of the Las Curtiembres Formation (Late Cretaceous, Salta Group Basin), Las Conchas Creek area, northwestern Argentina. Ameghiniana 45: 473–482.

Norbäck-Ivarsson L. 2014. Pollen morphology in *Ephedra* (Gnetales) and implications for understanding fossil ephedroid pollen from the Tibetan Plateau, using a phylogenetic approach. MSc thesis, Stockholm University, Stockholm, Sweden.

Ola-Buraimo AO. 2013. Biostratigraphy et paleoenvironment of deposition of Bima and Gongila formations in M-1 Well, Bornu Basin, northeastern Nigeria. International Journal of Scientific et Technology Research 2: 320–328.

Os K, Muller J, Waterbolk HTH. 1955. The application of palynology to oil geology with reference to western Venezuela. Geologie en Mijnbouw 17: 49–75.

Osborn JM, Taylor TN, De Lima MR. 1993. The ultrastructure of fossil ephedroid pollen with gnetalean affinities from the Lower Cretaceous of Brazil. Review of Palaeobotany and Palynology 77: 171–184.

Paytan A. 2012. Geochemistry. Mountains, weathering, and climate. Science 335: 810–811. doi:10.1126/science.1218342.

Pierce RL. 1961. Lower Upper Cretaceous Plant Microfossils from Minnesota. Bulletin 42: 1–82.

Pocock SAJ. 1964. Pollen and spores of the Chlamydospermidae and Schizaeaceae from Upper Mannville Strata of the Saskatoon area of Saskatchewan. Grana Palynologica 5: 129–209. doi:10.1080/00173136409430013.

Pocock SAJ, Vasanthy G. 1988. *Cornetipollis reticulata*, a new pollen with angiospermid features from Upper Triassic (Carnian) sediments of Arizona (USA), with notes on *Equisetosporites*. Review of palaeobotany and palynology 55 (4): 337–356.

Pons D. 1983. Contribution à l'étude paléobotanique du Mésozoïque et du Cénozoïque de Colombie. PhD dissertation. Université Paris VI, Paris, France.

Pons D. 1988. Le Mésozoïque de Colombie. Macroflores et microflores. Paris, France: Cahiers de Paléontologie, Centre national de la recherche scientifique.

Pons D, Berthou PY, Campos DEA. 1990. Quelques observations sur la palynologie de l'Aptien supérieur et de l'Albien du Bassin d'Araripe (N.E. du Bre´sil). Atas do I simpósio sobre a Bacia do Araripee Bacias interiores do nordeste, Crato, 241–252.

Pons D, Berthou PY, Filgueira JBM, Sampaio JA. 1994. Palynologie des unités lithostratigraphiques "Fundão","Crato" et "Ipubi"(Aptien Supérieur à Albien Infârieur-moyen, Bassin d'Araripe, NE du Brésil): Enseignements paléoécologiques, stratigraphiques et climatologiques. Géologie de l'Afrique et de l'Antique Sud. Compte-Rendu des Colloques de Géologie d'Angers 16: 383–401.

Potonié R. 1958. Synopsis der Gattungen der Sporæ dispersæ. II. Teil: *Sporites* (Nachträge), *Saccites*, *Aletes*, *Praecolpates*, *Polyplicates*, *Monocolpates*. Beihefte zum Geologischen Jahrbuch 31: 1–114.

Punt W, Hoen P, Blackmore S, Nilsson S, Le Thomas A. 2007. Glossary of pollen and spore terminology. Review of Palaeobotany and Palynology 143: 1–81. doi:10.1016/j.revpalbo.2006.06.008.

Quan C, Liu Y-S, Utescher T. 2011. Paleogene evolution of precipitation in northeastern China supporting the middle Eocene intensification of the East Asian monsoon. Palaios 26: 743–753. doi:10.2110/palo.2011.p11-019r.

Quan C, Liu Y-S, Utescher T. 2012. Eocene monsoon prevalence over China: A palaeobotanical perspective. Palaeogeography, Palaeoclimatology, Palaeoecology 365: 302–311. doi:10.1016/j.palaeo.2012.09.035.

Regali MSP, Uesugui N, Santos AS. 1974. Palinologia dos sedimentos meso-cenozóicos do Brasil (II). Boletim Técnico da Petrobrás 17: 263–301.

Regali MSP, Viana CF. 1989. Late Jurassic-Early Cretaceous in Brazilian sedimentary basins: Correlation with the International Standard Scale. Rio de Janeiro, Brazil: Petrobrás.

Rieser AB, Bojar A-V, Neubauer F, Genser J, Liu Y, Ge X-H, Friedl G. 2009. Monitoring Cenozoic climate evolution of northeastern Tibet: Stable isotope constraints from the western Qaidam Basin, China. International Journal of Earth Sciences 98: 1063–1075. doi:10.1007/s00531-008-0304-5.

Schrank E. 2010. Pollen and spores from the Tendaguru Beds, Upper Jurassic and Lower Cretaceous of southeast Tanzania: Palynostratigraphical and paleoecological implications. Palynology 34 (1): 3–42.

Schrank E, Mahmoud MS. 2000. New taxa of angiosperm pollen, miospores and associated palynomorphs from the early Late Cretaceous of Egypt (Maghrabi Formation, Kharga Oasis). Review of Palaeobotany and Palynology 112 (1): 167–188.

Scott RA. 1960. Pollen of *Ephedra* from the Chinle formation (Upper Triassic) and the genus *Equisetosporites*. Micropaleontology 6: 271–276. doi:10.2307/1484233.

Shakhmundes V. 1965. New species of *Ephedra* L., from Paleogene deposits of north-western Siberia. Transactions Vses, Nauchno-Issled Geologorazved Institute 239: 214–228.

Shaw C-L. 1998. Eocene ephedraceous palynomorphs of Taiwan. Botanical Bulletin of Academia Sinica 39: 69–80.

Sinanoglu E. 1984. Early Cretaceous palynomorphs from the Zuata area, eastern Venezuela. Boletim Instituto Geociências, Universidade de São Paulo 15: 116–128.

Singh C. 1964. Microflora of the lower Cretaceous Mannville Group, east-central Alberta. Research Council of Alberta Geology Division Bulletin, 15: 129–134.

Song B, Zhang K, Lu J, Wang C, Xu Y, Greenough J. 2013. The middle Eocene to early Miocene integrated sedimentary record in the Qaidam Basin and its implications for paleoclimate and early Tibetan Plateau uplift. Canadian Journal of Earth Sciences 50: 183–196. doi:10.1139/cjes-2012-0048.

Song Z. 1978. Early Tertiary spores and pollen grains from the coastal region of Bohai. Beijing: Science Press.

Song Z. 1999. Fossil spores and pollen of China: The Late Cretaceous and Tertiary spores and pollen. Beijing: Science Press.

Song Z, Wang W, Mao F. 2008. Palynological implications for relationship between aridification and monsoon climate in the Tertiary of NW China. Acta Palaeontology Sinica 47: 265–272.

Srivastava SK. 1968. Ephedralean pollen from the Upper Cretaceous Edmonton Formation of Alberta (Canada) and their paleoecological significance. Canadian Journal of Earth Sciences 5: 211–221. doi:10.1139/e68-022.

Staisch LM, Niemi NA, Hong C, Clark MK, Rowley DB, Currie B. 2014. A Cretaceous-Eocene depositional age for the Fenghuoshan Group, Hoh Xil Basin: Implications for the tectonic evolution of the northern Tibet Plateau. Tectonics 33 (3): 281–301.

Steeves MW, Barghoorn ES. 1959. The pollen of *Ephedra*. Journal of the Arnold Arboretum 40: 221–255.

Stover LE. 1964. Cretaceous ephedroid pollen from West Africa. Micropaleontology 10: 145–156. doi:10.2307/1484637.

Sun X, He Y. 1980. Study of spores and pollen grains from Paleocene Jiangxi Province. Beijing: Science Press.

Sun X, Wang P. 2005. How old is the Asian monsoon system? Palaeobotanical records from China. Palaeogeography, Palaeoclimatology, Palaeoecology 222: 181–222. doi:10.1016/j.palaeo.2005.03.005.

Sun X, Zhao Y, He Z. 1984. The Oligocene–Miocene palynological assemblages from the Xining-Minghe basin. Qinghai Province. Geological Review 30: 207–216.

Sung T, Tsao L. 1980. Fossil spores and pollen from the Fushun Group. Bulletin of the Institute of Mineral Deposits. Chinese Academy of Geological Sciences 7: 99–132.

Takahashi M, Takai K, Saiki K. 1995. Ephedroid fossil pollen from the Lower Cretaceous (upper Albian) of Hokkaido, Japan. Journal of Plant Research 108: 11–15. doi:10.1007/BF02344300.

Thiergart F. 1938. Die Pollenflora der Niederlausitzer Braunkohle. Jahrbuch der Preussischen Geologischen Landesanstalt zu Berlin 58: 282–351.

Upshaw CF. 1964. Palynological zonation of the Upper Cretaceous Frontier Formation near Dubois, Wyoming. Palynological Zonation of Frontier Formation 1: 153–168.

Vajda-Santivanez V. 1999. Miospores from upper Cretaceous–Paleocene strata in northwestern Bolivia. Palynology 23 (1): 181–196.

Van Ameron HWJ. 1965. Upper Cretaceous pollen and spores assemblages from the so-called "Wealden" of the province of Leon (northern Spain). Pollen et Spores 7: 93–133.

Wang D, Sun X, Zhao Y. 1990. Late Cretaceous to Tertiary palynofloras in Xinjiang and Qinghai, China. Review of Palaeobotany and Palynology 65: 95–104. doi:10.1016/0034-6667(90)90060-V.

Wang J, Fang X, Appel E, Song C. 2012. Pliocene–Pleistocene climate change at the NE Tibetan Plateau deduced from lithofacies variation in the drill core SG-1, western Qaidam Basin, China. Journal of Sedimentary Research 82: 933–952. doi:10.2110/jsr.2012.76.

Wang J, Wang YJ, Liu ZC, Li JQ, Xi P. 1999. Cenozoic environmental evolution of the Qaidam Basin and its implications for the uplift of the Tibetan Plateau and the drying of central Asia. Palaeogeography, Palaeoclimatology, Palaeoecology 152: 37–47. doi:10.1016/S0031-0182(99)00038-3.

Wang W-M, Shu J-W. 2013. Cenozoic xeromorphic vegetation in China and its spatial and temporal development in connection with global changes. Palaeoworld 22: 86–92. doi:10.1016/j.palwor.2013.08.001.

Wodehouse RP. 1933. Tertiary pollen-II. The oil shales of the Eocene Green River formation. Bulletin of the Torrey Botanical Club 60: 479–524. doi:10.2307/2480586.

Wodehouse RP. 1935. Pollen grains: Their structure, identification and significance in science and medicine. New York: Hafner.

Wu G, Liu Y, Dong B, Liang X, Duan A, Bao Q, Yu J. 2012. Revisiting Asian monsoon formation and change associated with Tibetan Plateau forcing: I. Formation. Climate Dynamics 39: 1169–1181. doi:10.1007/s00382-012-1334-z.

Wu Z. 1980. Vegetation of China. Beijing: Science Press.

Wu Z, Ye P, Hu D, Peng H. 2006. Late Cenozoic environmental evolution of the Qinghai-Tibet Plateau as indicated by the evolution of sporopollen assemblages. Geology in China 33: 966–979.

Xiao G, Abels HA, Yao Z, Dupont-Nivet G, Hilgen FJ. 2010. Asian aridification linked to the first step of the Eocene–Oligocene climate Transition (EOT) in obliquity–dominated terrestrial records (Xining Basin, China). Climate of the Past 6: 501–513. doi:10.5194/cp-6-501-2010.

Yang Y. 2002. Systematics and evolution of *Ephedra* L. (Ephedraceae) from China. PhD dissertation. The Chinese Academy of Science, Beijing, China.

Yang Y, Geng BY, Dilcher DL. et al. 2005. Morphology and affinities of an early Cretaceous *Ephedra* (Ephedraceae) from China. American Journal of Botany 92 (2): 231–241.

Yi S, Batten DJ. 2002. Palynology of Upper Cretaceous (uppermost Campanian–Maastrichtian) deposits in the South Yellow Sea Basin, offshore Korea. Cretaceous Research 23: 687–706. doi:10.1006/cres.2002.1032.

Yu J, Guo Z, Mao S. 1983. Cretaceous palynological assemblages from the district south of the Songhua River. Professional Papers of Stratigraphy and Palaeontology 10: 1–87.

Yu J, Zhang H, Lin Q, Gu Y, Zhang Z. 2003. Geological implications of *Sporopollenites* flora from Tertiary Xining Group in Minhe County, Qinghai Province. Earth Science Journal of China University of Geosciences 28: 401–406.

Zavada MS. 1990. The ultrastructure of three monosulcate pollen grains from the Triassic Chinle Formation, western United States. Palynology 14: 41–51.

Zhang W, Appel E, Fang X, Song C, Cirpka O. 2012. Magnetostratigraphy of deep drilling core SG-1 in the western Qaidam Basin (NE Tibetan Plateau) and its tectonic implications. Quaternary Research 78: 139–148. doi:10.1016/j.yqres.2012.03.011.

Zhang X, Sun S, Yong S, Zhou Z, Wang R. 2007. Vegetation map of the People's Republic of China (1: 1 000 000). Beijing: Geological Publishing House.

Zhang Y, Xi Y. 1983. Studies on the pollen morphology of Chinese *Ephedra*. Acta Botanica Sinica 25: 418–427.

Zhang Y, Zhan J. 1991. Late Cretaceous and Early Tertiary spores and pollen from the Western Tarim Basin, S. Xinjiang, China. Beijing: Science Press.

Zhu Z, Wu L, Xi P, Song Z, Zhang Y. 1985. A research on Tertiary palynology from the Qaidam Basin, Qinghai Province. Beijing: Petroleum Industry Press.

Table I. Reference list for Figure 1.

Name	Location	Age	Reference
Ephedroid pollen	Hokkaido, Japan Punjab, India SE Oregon NW Siberia Germany	Upper Albian Lower Miocene–Oligocene Miocene Paleogene Oligocene	15, 16, 30, 65, 73
Ephedra archaeorhytidosperma	Western Liaoning Province, northeast China	Early Cretaceous	77
Ephedra stapfii Steeves et Barghoorn 1959	Long Island, North America Juan Basin, New Mexico, Minnesota NE Texas, Western Alabama, Dubois, Wyoming, Oklahoma, Siberia, Northern Spain, Nigeria, Venezuela and Iran	Late Cretaceous	2, 7, 8, 19, 32, 33, 53, 71, 74, 76
Ephedripites ambonoides Brenner 1968	Peru	Albian–Cenomanian	5
Ephedripites barghoornii Pocock 1964	NE Brazil, Colombia	Albian–Cenomanian	20–25
Ephedripites brasiliensis Herngreen 1973	NE Brazil	Albian–Cenomanian	20, 21, 39
Ephedripites eocenipites (Wodehouse) Krutzsch 1961	Northern Taiwan	Eocene	66
Ephedripites elsikii Herngreen 1975	NE Brazil, Maranhão, Barreirinhas Basin	Cenomanian	22–24, 39
Equisetosporites huguesi Pocock 1964	Saskatoon, Saskatchewan	Middle–upper Albian	55
Ephedripites jansonii (Pocock 1964) Müller 1968	NW Bolivia Offshore Korea	Upper Cretaceous–Paleocene	75 79
Ephedripites megafusiformis Ke et Shi 1978	Western part of Eastern Kunlun, China	Eocene	18
Ephedripites montanaensis Brenner 1968	NW Bolivia	Upper Cretaceous–Paleocene	75
Ephedripites pentacostatus Brenner 1968	Peru, NE Brazil	Albian–Cenomanian	5, 35, 61
Ephedripites subtilis Regali, Uesugui et Santos 1974	NE Brazil	Cenomanian	39, 61
Ephedripites sulcatus Brenner 1968	Peru	Albian	5, 6
Ephedripites validus Brenner 1968	Peru	Albian	5
Ephedripites wolkenbergensis Krutzsch 1961	Southern margin of Laurasia, Xizang (Tibet)	Cretaceous–Eocene	33
Ephedripites (*Ephedripites*) sp.	NE Brazil, Suriname southeastern Australia South Hungary NW Argentina (Las Conchas Creek area) southern Alps, southern Switzerland, northern Italy	Aptian–Maastrichtian Paleocene–Eocene Miocene Neocomian Aptian–Albian Cenomanian	4, 10, 13, 21–23, 27, 48, 49, 50
Ephedripites sp.	Xining Basin, China Qaidam Basin,China Lanzhou Basin Fenghuoshan Group, Hoh Xil Basin	Eocene Miocene Cretaceous–Eocene	28, 46, 70
Ephedripites (*Distachya*) *sp.*	(Claiborne) Flora, Alabama Florida, USA southern Hungary	Eocene Middle Eocene Miocene	17, 29, 49
Equisetosporites albertensis Singh 1964	NE Brazil, Alagamar, Crato, Ipubi Fms.	Aptian–Lower Albian	11, 13, 35, 37–39, 59
Equisetosporites ambiguus Hedlund, 1966 in De Lima 1980	NE Brazil, Exu, Crato, Ipubi, Missão Velha, Rio Batateira Fms. Colombia, Venezuela	Aptian–Albian	35–38, 43, 56–59, 67

(*Continued*)

Table I. (*Continued*).

Name	Location	Age	Reference
Equisetosporites cancellatus Paden Phillips et Felix 1971	NE Brazil, Rio do Peixe	Neocomian	42
Equisetosporites chinleanus Daugherty 1941	USA, Chinle, Arizona, Circle Cliffs, Garfield County, Utah	Cretaceous	54 79
Equisetosporites concinnus Singh 1964	NE Brazil, Alagamar, Codó, Crato, Ipubi, Missão Velha, Rio Batateira Fms. SE Tanzania, East-central Alberta	Aptian–Albian; Lower Cretaceous Lower Cretaceous	11, 12, 35, 37, 40, 43, 59, 63, 68
Equisetosporites costaliferous (Brenner 1968) De Lima 1980	NE Brazil, Codó, Crato, Exu Fms.; Colombia, Peru	Aptian–Cenomanian	5, 35–40, 56, 57
Equisetosporites crenulatus De Lima 1981	NE Brazil; Crato, Exu Fms.	Aptian–Albian	35–37, 39
Equisetosporites dudarensis (Deák 1964) De Lima in Pons 1988	NE Brazil, Alagamar, Crato, Ipubi, Missão, Velha, Rio Batateira Fms. Colombia, Peru, Venezuela	Aptian–Cenomanian	5, 11, 12, 35, 37, 38, 44, 57, 59, 63
Equisetosporites elegans De Lima 1980	NE Brazil, Crato Fm.	Late Aptian–Lower Albian	35, 37–39
Equisetosporites elongatus (Horowitz 1966) De Lima 1982	NE Brazil, Codó, Crato Fms.	Aptian–Albian	11, 35, 37, 38, 40
Equisetosporites evidens (Bolkhovitina 1961) De Lima 1980	NE Brazil, Crato Fm.	Late Aptian–Lower Albian	35, 37, 38
Equisetosporites fragilis De Lima 1980	NE Brazil, Codó, Crato, Exu Fms.	Aptian–Albian	35–40
Equisetosporites huguesi Pocock 1964	NE Brazil, Crato, Exu Fms.	Aptian–Albian	35–38
Equisetosporites irregularis (Herngreen 1973) De Lima 1980	NE Brazil, Barreirinhas, Crato, Exu Fms.	Aptian–Cenomanian	20–24, 26, 35–38, 62
Equisetosporites lanceolatus De Lima 1980	NE Brazil, Crato, Exu Fms.	Aptian–Albian	35–39
Equisetosporites laticostatus De Lima 1980	NE Brazil, Alagamar, Crato, Exu Fms.	Aptian–Albian	12, 35, 36, 38, 39
Equisetosporites lawalii Schrank 2000	El-Kharga, Egypt	Cenomanian- Early Turonian	64
Equisetosporites leptomatus De Lima 1980	NE Brazil, Alagamar, Crato, Exu, Jatoba, Missão Velha, Rio Batateira Fms., Colombia	Aptian–Albian	12, 35–39, 41, 43, 56, 57, 59
Equisetosporites luridus De Lima 1980	NE Brazil; Alagamar, Crato, Missão Velha, Rio Batateira Fms.	Aptian–Albian	12, 35, 37, 38, 39, 43, 59
Equisetosporites maculosus Dino 1994	NE Brazil, Alagamar, Crato Fms.	Aptian–Lower Albian	13, 59
Equisetosporites minuticostatus De Lima 1980	NE Brazil, Alagamar, Codó, Crato, Ipubi, Missão Velha, Rio Batateira Fms.	Aptian–Albian	12, 35–40, 43, 59
Equisetosporites mollis Srivastava 1968	Colombia	Albian	56, 57
Equisetosporites notensis (Cookson 1957) Romero 1977	Otago, Southern New Zealand	Early Miocene (~ 23 Ma)	47
Equisetosporites ovatus (Pierce 1961) Singh 1964	NE Brazil, Alagamar, Crato, Exu, Ipubi, Missão Velha, Rio Batateira Fms., Rio do Peixe	Neocomian–Albian	12, 35–38, 42, 43, 59
Equisetosporites procerus (Brenner 1968) De Lima 1980	NE Brazil, Crato Fm., Peru	Aptian–Albian	5, 6, 38
Equisetosporites reyrei De Lima 1981	NE Brazil, Crato, Exu Fms.	Aptian–Albian	35–37, 39, 58
Equisetosporites strigatus (Brenner 1968) De Lima 1980	NE Brazil, Codó, Crato Fms., Colombia, Peru	Aptian–Albian	5, 35, 36, 38, 40, 67
Equisetosporites subcircularis De Lima 1980	NE Brazil, Codó, Crato, Exu Fms., Colombia	Aptian–Albian	35–40, 57, 58
Equisetosporites subcircularis De Lima 1980	NE Brazil, Codó, Crato, Exu Fms., Colombia	Aptian–Albian	35–40, 57, 58
Equisetosporites translucidus Deák et Combaz 1967	Colombia, Venezuela	Aptian–Albian	57, 67

(*Continued*)

Table I. (*Continued*).

Name	Location	Age	Reference
Equisetosporites virginiaensis Brenner 1968	NE Brazil, Rio do Peixe	Neocomian	42
Equisetosporites sp.	NE Brazil, Crato Fm.	Aptian–Albian	35, 38, 52
Gnetaceaepollenites barghoornii (Pocock 1964) De Lima 1980	NE Brazil, Alagamar, Crato, Exu, Ipubi, Missão Velha, Rio Batateira Fms.	Aptian–Albian	12, 20, 22, 35, 36, 38, 43, 44, 58, 59
Gnetaceaepollenites boltenhagenii Dejax 1985	NE Brazil, Rio do Peixe; Barreirinhas Basin, Crato, Ipubi, Missão Velha, Rio Batateira Fms., Colombia	Neocomian–Cenomanian	20, 42, 43, 57–59
Gnetaceaepollenites chlatratus Stover 1964	NE Brazil, Alagamar, Crato, Exu, Missão Velha Fms., Rio do Peixe;	Neocomian–Cenomanian	12, 35–38, 42, 43, 59, 61, 72
Gnetaceaepollenites clathratus Stover 1964	Bornu Basin, NE Nigeria	Albian–Cenomanian	51
Gnetaceaepollenites diversus Stover 1964	NE Brazil, Africa Tano basin, Ghana	Cenomanian Albian–Tutonian	3, 22–24, 26, 61, 72
Gnetaceaepollenites fissuratus (Paden-Phillips et Felix 1971) De Lima 1980	NE Brazil, Crato, Exu Fms.	Aptian–Albian	35–38
Gnetaceaepollenites jansonii (Pocock 1964) De Lima 1980	NE Brazil, Alagamar, Codó, Crato, Exu, Missão Velha, Rio Batateira Fms., Barreirinhas Basin	Upper Aptian–Cenomanian	12, 20, 24, 26, 35, 36, 38, 40, 42, 43, 44, 59
Gnetaceaepollenites lajwantis Srivastava 1968	NE Brazil, Rio do Peixe	Neocomian	42
Gnetaceaepollenites mollis (Srivastava 1968) De Lima 1980	NE Brazil, Alagamar, Crato Fms.	Aptian–Lower Albian	12, 35, 37, 38
Gnetaceaepollenites oreadis Srivastava 1968	NE Brazil, Codó, Crato, Exu Fms. Alberta	Aptian–Albian Upper Cretaceous	35, 36, 38, 40, 69
Gnetaceaepollenites ornatus De Lima 1980	NE Brazil, Crato, Exu Fms.	Aptian–Albian	35, 36, 38–40
Gnetaceaepollenites ovatus	Shikotan Island	Maastrichtian–Danian	45
Gnetaceaepollenites perforatus De Lima 1980	NE Brazil, Crato Fm., Colombia	Aptian–Albian	35, 37–39, 56
Gnetaceaepollenites retangularis De Lima 1980	NE Brazil, Codó, Crato Fms.	Aptian–Albian	2, 35, 37, 38, 40
Gnetaceaepollenites santosii De Lima 1980	NE Brazil, Alagamar, Crato Fms.	Aptian–Lower Albian	12, 35, 37–39
Gnetaceaepollenites uesuguii De Lima 1980	NE Brazil, Crato, Exu Fms., Rio do Peixe	Neocomian–Albian	11, 12, 35–39, 42
Gnetaceaepollenites undulatus (Regali et al. 1974) De Lima 1980	NE Brazil, Crato, Exu, Missão Velha Fms.	Aptian–Cenomanian	12, 35–38, 43, 59, 61
Gnetaceaepollenites sp.	NE Brazil, Crato Fm., Suriname NW Argentina (Las Conchas Creek area) Gongola Basin, Nigeria El-Kharga, Egypt Urengoy, Russia	Aptian–Turonian Neocomian Cenomanian Aptian–Cenomanian	1, 4, 8, 9, 11, 35, 37, 38, 50, 64
Regalipollenites De Lima 1980	NE Brazil	Upper Aptian–Middle Albian (type species)	14, 35, 38
Regalipollenites amphoriformis (Regali et al. 1974) De Lima 1980	NE Brazil, Alagamar, Crato, Missão Velha Fms., Barreirinhas Basin, Ecuador	Upper Aptian–Middle Albian	12, 14, 35, 37, 38, 43, 59, 61
Singhia Srivastava 1968	Africa	Cretaceous (type species)	69
Singhia acicularis De Lima 1980	NE Brazil, Crato Fm.	Aptian–Albian	35, 37–39
Singhia crenulata De Lima 1980	NE Brazil, Alagamar, Crato Fms.	Aptian–Lower Albian	12, 38
Singhia elongata (Horowitz 1970) De Lima 1980	NE Brazil, Alagamar, Crato Fms.	Aptian–Lower Albian	12, 38

(*Continued*)

Table I. (*Continued*).

Name	Location	Age	Reference
Singhia minima De Lima 1980	NE Brazil, Codó, Crato Fms.	Aptian–Albian	35, 37–40
Singhia montanaensis (Brenner 1968) De Lima 1980	Peru, NE Brazil, Codó, Crato, Exu Fms.	Aptian–Cenomanian	5, 35–38, 40
Singhia multicostata (Brenner 1968) De Lima 1980	NE Brazil, Alagamar, Crato Fms.	Aptian–Lower Albian	11, 35, 37, 38
Singhia minima De Lima 1980	NE Brazil, Exu, Crato Fms.	Aptian–Albian	35–39
Singhia punctata De Lima 1980	NE Brazil, Crato Fm.	Upper Aptian	35, 37–39
Singhia reyrei De Lima 1980	NE Brazil, Crato Fm.	Upper Aptian	11, 38
Steevesipollenites Stover 1964	Africa	Cenomanian–Turonian (type species)	72
Steevesipollenites alatiformis Regali et al. 1974	NE Brazil	Albian	39, 61
Steevesipollenites binodosus Stover 1964	Africa, NE Brazil, Crato, Exu Fms., Sergipe et Barreirinhas Basins, Gongola Basin, Nigeria Bornu Basin, NE Nigeria	Aptian–Cenomanian	1,20–23, 35–38, 51, 61, 72
Steevesipollenites cupuliformis Azéma & Boltenhagen 1974	NE Brazil, Alagamar, Codó, Crato Fms.	Aptian–Albian	12, 35, 37, 38, 40
Steevesipollenites dayani Brenner 1968	Peru, NE Brazil, Crato, Exu Fms.	Albian–Cenomanian	5, 6, 35, 36
Steevesipollenites duplibaculum Regali et al. 1974	NE Brazil	Albian–Cenomanian	39, 61
Steevesipollenites giganteus Regali et al. 1974	NE Brazil	Cenomanian	39, 61
Steevesipollenites grambasti Azéma et Boltenhagen 1974	NE Brazil, Codó, Crato, Exu Fms.	Aptian–Albian	35–38, 40
Steevesipollenites multilineatus Stover 1964	Africa, NE Brazil	Albian–Cenomanian	20, 23, 24, 26, 72
Steevesipollenites nativensis Regali et al. 1974	NE Brazil	Cenomanian	61
Steevesipollenites patapscoensis (Brenner 1963) De Lima 1980	NE Brazil, Crato, Exu Fms.	Aptian–Albian	35–38
Steevesipollenites pygmeus Azéma & Boltenhagen 1974	NE Brazil, Crato, Exu Fms.	Aptian–Albian	35–38
Steevesipollenites sp.	NE Brazil, Crato Fm. SE Tanzania	Aptian–Albian, Lower Cretaceous	35, 37, 38, 44, 63

References: 1, Abubakar et al. (2011); 2, Anderson (1959); 3, Baltes (1966); 4, Belsky et al. (1975); 5–6, Brenner (1968, 1976); 7, Brown and Pierce (1962); 8, Chlonova et al. (1994); 9, Chlonova et al. (1961); 10, Cookson (1956); 11, Crane and Maisey (1991); 12–13, Dino (1992, 1994); 14, Dino et al. (1999); 15, Ghosh et al. (1963); 16, Graham (1965); 17, Gray (1960); 18, Guo et al. (2006); 19, Hedlund (1966); 20–23, Herngreen (1973, 1974, 1975, 1981); 24, Herngreen and Chlonova (1981); 25, Herngreen and Duenãs Jimenez (1990); 26, Herngreen et al. (1996); 27, Hochuli (1981); 28, Hoorn et al. (2012); 29, Jarzen and Dilcher (2006); 30, Kirchheimer (1950); 31, Krutzsch (1961); 32, Kuyl et al. (1955); 33, Leopold and Pakiser (1964); 34, Li et al. (2008a); 35–41, De Lima (1978a, 1978b, 1979b, 1980, 1981, 1982, 1984); 42, De Lima and Coelho (1987); 43, De Lima and Perinotto (1984); 44, Mabesoone and Tinoco (1973); 45, Markevich et al. (2012); 46, Miao et al. (2013b); 47, Mildenhall et al. (2014); 48, Müller (1966); 49, Nagy (1963); 50, Narváez and Sabino (2008); 51, Ola-Buraimo (2013); 52, Osborn et al. (1993); 53, Pierce (1961); 54, Pocock and Vasanthy (1988); 55, Pocock (1964); 56–57, Pons (1983, 1988); 58–59, Pons et al. (1990, 1994); 60, Potonié (1958a); 61, Regali et al. (1974); 62, Regali and Viana (1989); 63, Schrank (2010); 64, Schrank and Mahmoud (2000); 65, Shakhmundes (1965); 66, Shaw (1998); 67, Sinanoglu (1984); 68, Singh (1964); 69, Srivastava (1968); 70, Staisch et al. (2014); 71, Steeves and Barghoorn (1959); 72, Stover (1964); 73, Takahashi et al. (1995); 74, Upshaw (1964); 75, Vajda-Santivanez (1999); 76, Van Ameron (1965); 77, Yang et al. (2005); 78, Yi and Batten (2002); 79, Zavada (1990).